AD NUMBER

AD813619

NEW LIMITATION CHANGE

TO

Approved for public release, distribution unlimited

FROM

Distribution authorized to U.S. Gov't. agencies and their contractors; Critical Technology; JAN 1967. Other requests shall be referred to Air Force Materials Lab., Wright-Patterson AFB, OH 45433.

AUTHORITY

USAFML ltr, 29 Mar 1972

AFML-TR-66-39

RESEARCH ON THE ROLE OF STRAIN RATE AND TEMPERATURE IN FATIGUE

NICHOLAS J. GRANT
JOSEPH T. BLUCHER
DONALD L. RITTER

MASSACHUSETTS INSTITUTE OF TECHNOLOGY

TECHNICAL REPORT AFML-TR-66-39

JANUARY 1967

AIR FORCE MATERIALS LABORATORY
RESEARCH AND TECHNOLOGY DIVISION
AIR FORCE SYSTEMS COMMAND
WRIGHT-PATTERSON AIR FORCE BASE, OHIO

NOTICES

When Government drawings, specifications, or other data are used for any purpose other than in connection with a definitely related Government procurement operation, the United States Government thereby incurs no responsibility nor any obligation whatsoever; and the fact that the Government may have formulated, furnished, or in any way supplied the said drawings, specifications, or other data, is not to be regarded by implication or otherwise as in any manner licensing the holder or any other person or corporation, or conveying any rights or permission to manufacture, use, or sell any patented invention that may in any way be related thereto.

Copies of this report should not be returned to the Research and Technology Division unless return is required by security considerations, contractual obligations, or notice on a specific document.

400 - March 1967 - C0192-26-585

RESEARCH ON THE ROLE OF STRAIN RATE AND TEMPERATURE IN FATIGUE

NICHOLAS J. GRANT
JOSEPH T. BLUCHER
DONALD L. RITTER

FOREWORD

This report was prepared by the Massachusetts Institute of Technology, Cambridge, Massachusetts, under USAF Contract No. AF33(615)-1143, Project No. 7351, "Metallic Materials," Task No. 735106, "Behavior of Metals". The work was administered under the direction of the Air Force Materials Laboratory, Research and Technology Division, Wright-Patterson Air Force Base, Ohio, with D. M. Forney acting as project engineer.

This work summarizes research on the role of strain rate and temperature in fatigue, which was initiated in 1963, and concluded in September, 1965. The manuscript was released by the authors in December, 1965, for publication as an AFML Technical Report.

The report was prepared under the direction of Professor Nicholas J. Grant, Department of Metallurgy, by Joseph T. Wlucher and Donald L. Ritter.

This technical report has been reviewed and approved.

W. J. TRAPP
Chief, Strength and Dynamics Branch
Metals and Ceramics Division
Air Force Materials Laboratory

ABSTRACT

This study is concerned with the roles of strain rate and temperature on fatigue behavior. For the purposes of the immediate work pure aluminum and an aluminum - 10 percent zinc alloy were selected. To simplify analyses of the observed behavior, an axial fatigue machine was designed to eliminate strain rate and stress gradients in the specimen cross-section. Strain rates of 5 and 150 percent per minute, strains of ± 1 percent, and temperatures from 80 to 900°F were the variables studied. A number of grain sizes were utilized to evaluate the role of alloy structure. Other strain rates, strains and structures, including two phase systems, are being examined to extend the studies. Thermal fatigue behavior will be examined and the results compared with the present observations in mechanical fatigue.

CONTENTS

ILLUSTRATIONS

ILLUSTRATIONS (Cont.)

ILLUSTRATIONS (Cont.)

INTRODUCTION

One often sees in the literature references to "high temperature fatigue", which, if closely examined, more correctly should refer to "fatigue at elevated temperatures". Fatigue studies carried out on conventional equipment (1000 to 10,000 rpm) encounter strain rates from about 1000 percent per minute to 250,000 depending on machine speed and strain amplitude. Even at very high temperatures high strain rates led only to work hardening of the structure, with little or no attendant recovery of the structure during the straining period. In fact, unless deformation modes identifiable with high temperature, low strain rate processes can occur, the fatigue behavior is controlled by the cumulative cold work which takes place.

The number of studies which have been undertaken of fatigue behavior at very low strain rates, for example, from 0.1 to 1000 percent per minute, is relatively small. At such low strain rates high temperature modes of deformation and fracture are evident at progressively higher temperatures. Grain boundary shear, grain boundary migration, subgrain formation, folding, etc., are discernable and indicative of high temperature deformation processes, which ultimately result in failure by an intergranular mechanism. In all these cases recovery and/or recrystallization processes are operative to counteract the strain hardening which occurred during any portion of a fatigue cycle.

It appeared desirable, under the circumstances, to examine fatigue behavior in greater detail as a function of strain rate, temperature, and structural variables to better understand the behavior of materials.

To avoid, at least initially unusually long time tests, and to establish a base line of observations for later comparisons, it appeared judicious to work at relatively high strains, but at low strain rates, over a very wide temperature range. Initially a strain of $\pm$ 1 percent was chosen at strain rates of 5 and 150 percent per minute. These conditions for aluminum and its alloys, based on other temperature - strain rate studies, were expected to involve low temperature type deformation at room temperature and higher, and at high temperature modes of deformation and fracture above about 500°F (where recovery, recrystallization and intergranular cracking could occur).

Prediction of the anticipated behavior patterns was based on extensive creep studies over a comparable temperature range and an extremely wide range of strain rates.

The initial studies were concerned with high purity aluminum and an aluminum-10 percent zinc alloy of equal basic purity. One phase of the program was concerned with mechanical behavior and the macroscopic aspects of deformation and fracture. A second phase was concerned with the microscopic details of deformation and fracture, undertaken to establish the modes of deformation and recovery, and the steps leading to the initiation of cracking and its progress to failure. Interrupted tests were a common feature of the latter phase of the study.

Both higher and lower strain rates, at higher and lower strains, are planned in order to extend our knowledge of fatigue behavior over a wide range of strain rates; temperature range of interest will continue to be from 80 to 900°F. As soon

as an adequate strain rate - temperature base is established for the materials of interest, thermal fatigue studies will be initiated. To make a meaningful comparison between mechanical and thermal fatigue behavior, strain rates, strains, and temperatures must be rigorously defined in terms of the observed modes of deformation and fracture. Since thermal fatigue requires the use of temperature, the effect of $T_{max.}$ must be known for its effect on structure and strain rate. Similarly, since there is a practical restriction on the range of strain rates which can be achieved in thermal fatigue, there must be an equivalent counterpart in mechanical behavior. It is expected that these comparisons can be made.

I. LOW STRAIN RATE FATIGUE BEHAVIOR OF ALUMINUM AS A FUNCTION OF TEMPERATURE

In high temperature deformation, the prime variables are temperature and strain rate. The higher the strain rate, the higher the temperature must be in order for recovery processes to occur, and for intercrystalline fracture to initiate and progress. In fact, if the strain rate is extremely high, high temperature deformation and recovery processes are prevented from occurring and conditions of slip and work hardening control, leading to transgranular fracture. This large role played by strain rate in deformation and fracture at elevated temperatures becomes extremely important in fatigue behavior. The use of conventional fatigue testing machines is an important factor in high temperature fatigue studies because the machines were built to permit completion of tests in a reasonable period of time; the resultant high strain rates (regardless of strain) cause the test material to work harden even at very high temperatures. For these studies, a machine capable of operating at low strain rates over a wide temperature interval was chosen to control the important test variables.

Because strain rate is the important variable, the existence of a wide spectrum of strain rates in each fatigue cycle would complicate interpretation of material behavior; accordingly, the test machine was built to provide axial deformation.

Materials and Experimental Procedure

Aluminum of better than 99.99% purity and an aluminum - 10 weight percent zinc alloy of comparable impurity content were selected for the study. The compositions in weight percent are indicated below:

99.99+ Al	Al - 10% Zn
0.003 Cu	0.001 Cu
0.001 Fe	0.001 Fe
0.002 Si	0.002 Si
0.001 Mn	0.001 Mn
99.99 Al	10.01 Zn
	balance Al

These materials have been studied extensively for deformation and fracture characteristics over the temperature range from 70 to 1150°F (1-6). Grain boundary sliding and migration have been investigated quantitatively for these materials over an equally wide temperature range (6,7).

Button-head specimens, with a liberal fillet of 0.20" diameter and of gauge length 0.40, were machined from wrought recrystallized bar stock. The ratio of 2:1 gauge length to gauge diameter was selected after preliminary tests sh-

that there was an effect of shorter gauge length, probably due to end effects, and after evidence of buckling in longer gauge length specimens. The specimen dimensions are shown in Figure 1.

After machining, the specimens were chemically polished to remove the worked outer layer, and were subsequently heat-treated to stabilize the selected grain sizes.

Both the high purity aluminum and the aluminum 10 percent zinc alloy were heat-treated to produce grain diameters of approximately 0.5 and 2 mm in each case. These grain sizes are referred to in the text as a fine and coarse grain, respectively. One lot of the high purity aluminum was heat-treated to produce an extremely coarse grain size in which the cross section was occupied by 2 to 3 grains. This structure is referred to as very coarse grained. After heat-treatment, the specimens again underwent an electrochemical polishing step, during which the shoulder and head of the specimens were protected with an insulating lacquer.

Test temperatures varied from 70° to 900°F. The strain amplitude in all of the reported tests was $\pm$ 1 percent, or a total strain amplitude of 2 percent. Constant strain rates of 5 and 150 percent per minute were selected so that grain boundary sliding and migration, subgrain formation, and fold formation would be operative in the higher temperature tests (1,2). The strain rates are nominal values due to the fact that they are based on the original dimensions of the specimen, and these dimensions changed significantly in many of the tests as will be observed from the photographs.

For the elevated temperature tests, a thermocouple was inserted into a well in the head of the specimen; the selected temperatures could be maintained with less than $\pm$ 5° F fluctuation during the entire test. To avoid complicating effects of time and temperature on structure, care was taken to bring the specimens to the test temperature as quickly as possible, in particular to avoid changes in grain size specimens were cooled to room temperature after fracture with an air blast to prevent recovery from occurring during cooling.

During the actual test, the load was constantly monitored as a function of time and recorded through a strain gauge load cell. Since these are constant strain rate tests, the recorded "load versus time" curves can be viewed as "load versus strain" curves. One recorder registered the load throughout the entire test period, yielding an envelope of load amplitude as a function of time; the other recorder registered the detailed shape of the individual load versus time cycle.

Typical load versus time curves are shown in Figures 2 and 3 at room temperature and 500°F for high purity aluminum, at a strain rate of 5 percent per minute, and at room temperature and 300°F for the coarse grained aluminum - 10 percent zinc alloy at a strain rate of 5 percent per minute. The presence or absence of strain hardening effects is clearly visible from curves of this sort. Figure 4 shows the recorded variation of load amplitude as a function of the percentage of total life for the high purity, coarse grained aluminum. Figure 5 shows a similar plot for the coarse grained aluminum - 10 percent zinc alloy. It is clear that work hardening is a minor factor in these low strain rate tests above 500°F for high purity aluminum, and above 300°F for the aluminum - zinc alloy.

To serve as a reference, tension tests were run for the several different grain sizes in each of the materials; the results are plotted in Figure 6. The tensile strength and reduction of area values are shown as a function of test temperature.

It is noted that the high purity aluminum shows virtually 100 percent reduction of area at all test temperatures, whereas the aluminum - zinc alloy achieves this status at about 500°F. Note the very low ductility exhibited in tests at room temperature and 300°F by the coarse grained aluminum - zinc alloy as a result of aging embrittlement due to preferential precipitation on the grain boundaries. The zinc strengthens aluminum significantly, but in the process the grain boundaries become relatively weak and brittle compared to the grains. Thus, at room temperature, the fine grained aluminum - zinc alloy showed a mixture of trans- and intergranular fracture modes; the coarse grained aluminum - zinc alloy showed only intercrystalline fractures. It was expected that this differential in strength and ductility between grains and grain boundaries would play an important role in the fatigue behavior of this alloy.

All surfaces were examined by means of an optical microscope directly, and then through a replicating technique utilizing amyl acetate film, which was then flattened and subjected to aluminum shadowing to improve contrast for viewing. Metallographic studies were combined with Laue back-reflection X-ray studies to establish the structural changes which had occurred during the course of any fatigue test.

Results

Figures 7 to 11 are plots of cycles to failure versus temperature at the two strain rates for the two materials, and for the several grain sizes investigated. In many instances, duplicate tests were run in order to establish reproducibility.

Figure 7 shows the results for fine grained high purity aluminum. The effect of the higher strain rate is to increase the cycles to failure above about 500°F, the effect becoming larger with increasing temperature, reaching a maximum between 700 and 800°F.

Figure 8 plots the results for coarse-grained high purity aluminum. The effect of increased strain rate is again small up to about 500°F. The coarse grained material sustains significantly higher cycles to failure below 500°F compared to the fine grained pure aluminum; this is an unexpected behavior. Above about 500°F, the number of cycles to failure increases with increasing temperature, reaching a maximum at about 600°F at the lower strain rate, and at 800°F at the higher strain rate.

Figure 9 shows the results for the extremely coarse grained high purity aluminum; the shapes of the curves are similar to those observed in Figure 8, with the same general trends as a function of temperature and strain rate. The very coarse grained structure sustains higher cycles to failure below 500°F than do the two smaller grained materials. The higher life of the coarser grained structure is unexplainable. Scatter of data appears to be more severe for the coarser grain sizes.

Figure 10 is a similar plot for the fine grained aluminum - 10 percent zinc alloy. At room temperature, the slower strain rate results in a shorter life to failure; this is also true above about 600°F. Point scatter, however, is such as to discourage conclusions other than at 80, 700, and 800°F. The general trends are similar to those observed for fine grained high purity aluminum, Figure 7, but are less clearly defined.

In Figure 11, the coarse grained aluminum - 10 percent zinc alloy shows extremely short life in the slower strain rate tests; the higher strain rate tests appear to lead to longer life both at room temperature, and again above about 600°F, as was the case with the fine grained structure, see Figure 11. The fine grained material shows less scatter of data and generally shows superior life to the coarse grained alloy. The embrittlement of the grain boundary in the coarse grained alloy is probably a factor.

Figure 12 shows photographs of failed specimens as a function of temperature, based on a strain rate of 5 percent per minute. Fracture are shown for fine and coarse grained high purity aluminum, and fine and coarse grained aluminum - 10 percent zinc. The macro-appearance of the deformation and fracture patterns will be discussed below.

Figures 13 to 16 show a series of photomicrographs for high purity aluminum illustrating the modes of deformation observed as a function of temperature, strain rate, and cycles of fatigue.

Figure 13 illustrates the very rapid accumulation of slip bands as a function of the number of cycles of fatigue strain. Even after one-half cycle (one percent strain), there is heavy slip concentration with a small amount of cross slip. No significant activity at the grain boundaries is observed. After 10 cycles, extensive cross slip has occurred; there is a profusion of deformation bands; and kinking occurs in many parts of the structure. After 100 cycles, in spite of the absence of significant grain boundary reaction, a number of intercrystalline cracks are observed (view c, Figure 13). The formation of intergranular cracks is unusual if one recalls that intergranular cracking has never been observed in aluminum of this purity in simple creep tests from room temperature to 1150°F (1).

The changes observed at 300 and 500°F are a general coarsening of the slip band spacing, and a small but definite indication of grain boundary shear, but with almost no grain boundary migration even at 500°F.

At 600°F, as observed in Figure 14, there is the first clear-cut evidence of both grain boundary sliding and grain boundary migration; and folds are noted in significant quantities for the first time. In comparing specimens with the 5 and 150 percent per minute rates, it is observed that the amount of grain boundary sliding and migration is considerably greater in the slow strain rate test, and slip band formation is absent to a significant extent in many of the grains due at the slower strain rate. Associated with grain boundary sliding, at least three large folds are observed in Figure 14 b. Referring to Figure 8, it is at 600°F that the first significant difference in life is observed for specimens tested at the two different strain rates. It is also at 600°F and above that the fracture changes for these coarse grained specimens (see Figure 12 b).

At 800°F (see Figure 15), after 10 cycles of fatigue strain, one observes large amounts of grain boundary migration in the slower strain rate tests, combined with the formation of serrated grain boundaries. By comparison, the higher strain rate tests (Figure 15 a) show more limited grain boundary migration. Specimens at both strain rates show coarse slip band spacing and frequent deformation bands.

An interesting deformation and recovery process is illustrated in Figure 16 for coarse grained pure aluminum tested at 800°F at a strain rate of 5 percent per minute. View A shows the microstructure before the start of the test, with identification markers. After two cycles of fatigue, there is significant grain boundary

sliding and migration; slip bands are barely visible. After 20 cycles, grain boundary migration has become very extensive with the grain boundaries tending to assume 45° directions. In view C this occurs by the gradual absorption of the smaller grain by the large ones with the triple points migrating along grain folds. After 100 cycles, the smaller grains in the region have been completely swept by migrating grain boundaries, eliminating these small grains from the structure, with the formation of grain boundaries at 45° directions to the axis of the specimen. This behavior brings about quadruple points on the surface. If reference is made to Figure 12, it will be observed that cracking in the 800° and 900° test is along these migrated 45° boundaries. This will be discussed in greater detail below.

Figure 17 shows the fatigue deformation of coarse-grained aluminum - 10 percent zinc alloy at a strain rate of 5 percent per minute at 80° and 300°F. Reference to Figure 11 shows that this alloy had a very small number of cycles to failure at 80°F. From Figure 12 D, it is evident that this alloy failed in a brittle intergranular manner with little or no prior deformation. This was also the case for the fine-grained aluminum - 10 percent zinc alloy. In fact, Figure 17 shows that after 10 cycles of fatigue at 80°F, unexpectedly, fold formation occurs due to grain boundary sliding. The extent of slip is quite restricted (compare to Figure 13 b. The presence of a fine hard zinc precipitate in this structure leads to a relative strengthening of the grain out of proportion to the strengthening at the grain boundaries, as was evidenced by intergranular fractures at 80°F (see also Figure 6). Apparently the boundaries are not only brittle, but they are relatively weaker than the granular material, leading to the observed grain boundary sliding and infrequent fold formation, wherever a grain offers a convenient geometry for slip.

On increasing the temperature to 300°F, the system is over-aged, leading to a significant increase in cycles to failure. Figure 17 b now shows (at 300°F) heavier slip, but the fracture remains largely intergranular; note the grain boundary cracks in Figure 17 b. At 500°F and above, this alloy is again in the single phase field, and now the behavior is similar to that of pure aluminum, because zinc is a poor strengthener at these high temperatures. At 700°F, there is increased grain boundary sliding with limited grain boundary migration and a virtual absence of slip band formation. At 800°F, after 100 cycles, one observes abundant grain boundary sliding, absence of slip band formation, and clear-cut subgrain formation in the grain structure. Again, boundaries migrate to 45° positions; as Figure 12 shows, fractures at 800° are along the migrated boundaries in 45° positions to the specimen axis.

Discussion

Referring to Figures 7 to 12, and supplementing this with the metallographic observations in Figure 13 to 17, one observes major changes in both the mechanisms of deformation and fracture. The deformation and fracture characteristics are highly sensitive to strain rate, temperature, grain size, and composition. Essentially, three major zones are definable in terms of the deformation and fracture mechanisms as a function of the test temperature. Supporting evidence is obtained from a study of the macro-fractures observed in Figure 12.

1. From 80 - 500°F:

In the temperature interval from room temperature to approximately 500°F, depending on the strain rate, deformation, both in the 99.99% Al and in the aluminum - 10 percent zinc specimens, is dominated by slip and kinking in the grains without

grain boundary shear. An exception is the behavior of the aluminum - 10 percent zinc alloy at room temperature where, because of aging effects, it exhibits significant deformation on the grain boundaries. Below 500°F, when fractures are ductile, the specimens failed by a combination of a particular type of necking, so-called "cyclic strain induced creep", and by transcrystalline fatigue crack propagation. It is probable that slower strain rates than 5 percent per minute will bring about more high temperature deformation below 500°F.

For pure aluminum, as early as 10 percent of the total life of the specimens, intercrystalline cracks were observed to form randomly on the surface of the specimens; these cracks did not appear to propagate significantly either in depth or in width with increasing cycles of test. They did appear to serve as focal points for the subsequent transgranular cracking which occurred. In this temperature range, heavy deformation and subgrain formation were observed in the 99.99% Al specimens, as is indicated in Figures 18 and 23. The same thing is noted in the case of the aluminum - 10 percent zinc specimens above about 300°F, where the alloy is in the one-phase solid solution field.

Figure 23 compares Laue back-reflection pictures for pure aluminum and aluminum - 10 percent zinc, both tested for a comparable number of cycles at room temperature. Note the severe granular breakdown in the pure aluminum specimen and its absence in the aluminum - 10 percent zinc. Compare these results with the metallographic views, Figures 13 a and 17 a.

2. From 500 to 700°F:

Above about 500°F, but particularly at 700°F, grain boundary sliding, fold formation, and grain boundary migration become important; deformation and fracture become strongly strain-rate sensitive.

The advent of intergranular cracking results in decreased ductility at fracture (see Figure 12); however, the life of the specimens continued to increase largely because of the recovery action associated with migrating grain boundaries and subgrain formation. At 600°F fine microcracks are observed in a polished section along slip planes, passing from one grain to another in one instance (see Figure 19); other cracks stop at grain boundaries. Final failure is by an intergranular mechanism.

3. Above 700°F:

At 800 and 900°F, depending on grain size, but especially upon strain rate, the major observed change was the now extremely rapid and extensive migration of boundaries to 45° positions relative to the strain axis; this sets up conditions leading to easy boundary shear. Having migrated into the 45° position, the boundaries appeared unable to migrate to new unstrained positions, and fractures now changed completely to the intergranular variety, with cracks prevalent from shoulder to shoulder in the gauge length (see Figure 12). Void formation increased from 700 to 900°F. At 700°F little grain growth occurred, and the grains were heavily broken down to a fine sub-structure as observed in Figure 20 a. At 800°F, at the slower strain rate, voids were larger and more numerous, and the sub-structure was quite coarse (see Figure 20 b); note the quadruple point in Figure 20 b.

In these very high temperature tests, failures appear to start at the surface of the specimen, with gradual progression along the grain boundaries. The voids are not at the surface but are located well below and on cracked grain boundaries. Figure 21 shows the interior of a failed specimen after testing at 700°,

and Figure 22 shows the 45° cracking of an aluminum - 10 percent zinc alloy after testing at 800°F.

The role of strain rate becomes significant above about 500 or 600°F, where grain boundary sliding and migrations begin to be significant. A change from 5 to 150 percent per minute tends to increase the number of cycles to failure above 500°F. This effect is smaller in the case of high purity aluminum, and is quite large in the case of the aluminum - 10 percent zinc alloy, shifting the temperature at which maximum life occurs by a significant amount.

Three observations deserve repeating:

1. There is the observation of intergranular cracking in very pure aluminum at 80°F. No combination of temperature and strain rate has produced intergranular cracks in aluminum of this purity in simple tension or torsion, nor in fatigue to the authors' knowledge.

2. There is the limited slip and enhanced grain boundary shear at room temperature observed for aluminum - 10 percent zinc alloys, with subsequent intergranular failure. It is uncommon for an aluminum alloy to exhibit grain boundary shear and fold formation at 80°F.

3. There is the unusual migration of grain boundaries to 45° positions relative to the deformation axis of the specimen, and the assumption of quadruple points, which leads to severe 45° intergranular failure at and above 800°F. Under creep conditions for comparable temperatures and strain rates, the tendency is for grain boundaries to migrate to a position nearer 90° to the strain axis, thereby offering maximum resistance to shear under stress. Coupled with such migrated and pinned 45° grain boundaries is the heavy void formation and intergranular cracking, neither of which occur in simple creep for any combination of strain rate and temperature.

II. MICROSCOPIC ASPECTS OF DEFORMATION AND FRACTURE OF ALUMINUM AS A FUNCTION OF STRAIN RATE AND TEMPERATURE IN AXIAL FATIGUE

Materials and Experimental Procedure

Utilizing in part the fractured test specimens described in the first section of the report, and supplementing them with tests interrupted at various time intervals, detailed studies have been undertaken to examine the modes of deformation which prevail, the origin of cracks, and the progression of cracks to failure. The variables are: temperature (80 to 900°F), strain rate (5 and 150 percent per minute), strain amplitude ($\pm$ 1 and $\pm$ 2 percent), grain size and grain orientation. In all cases the material was aluminum of greater than 99.99 percent purity.

Using button-head test specimens, it was a simple matter to interrupt tests, make measurements, or perform metallographic and X-ray diffraction studies, then return the specimen to test.

In all cases the test specimen was initially chemically and electrolytically polished to remove worked material and to permit etching to delineate all grain boundaries. Tests were interrupted after 1/4, 1/2, 1, 2, 10, 50, etc., cycles in the course of this study.

Both light and electron microscopy have been utilized. Because round specimens are used, a surface replicating technique was adopted using a plastic film

which could be flattened for observation. For light microscopy, the film was shadowed by evaporation of a thin layer of metal, for example, aluminum. For the electron microscope, because of severe surface rumpling and large grain boundary offsets, magnifications were limited to 600 to 3500X. It was necessary to devise a very coarse specimen holding grid, and replicas had to be large compared to the grid opening and strong enough to support their own weight without sagging. Replicas about 1/8" square, with heavy deposits of chromium and carbon, were used to obtain the desired strength. The most successful shadowing was accomplished at 45° to the tension direction, turning the specimen 90°, and shadowing again. Because both grain and grain boundary shear tend to take place close to the 45° directions, this gave the best contrast.

An effort is being made to examine replicas with an interferometric microscope. Using interference contrast and polarized light, this microscope gives a clearer picture of the specimen surface, which is observed by comparing Figures 26 and 28 the former was taken on the latest Leitz-Wetzlar metallograph with the diaphragm almost fully closed.

Results

Interrupted tests have thus far been run at 300, 500, 650, and 800°F, following deformation progress generally, and at 650 and 800°F for a more detailed examination of grain boundary shear and migration. Strains of $\pm$ 2 percent are included to compare against strains of $\pm$ 1 percent.

In an effort to decrease slip at higher temperatures, finer grained specimens are also being tested so that more grain boundaries can be studied at 300 and 500°F.

Following the work of Brunner and Grant (7) and Mullendore and Grant (6) on quantitative studies of grain boundary shear and migration during creep, similar studies are now beginning under fatigue conditions. For this purpose complete orientation charts have been prepared of coarse grained test specimens for which the orientation of each grain has been measured, as well as the grain boundary orientation. Mullendore and Grant had shown that the resolved critical shear stress for slip did not determine the amount of grain boundary sliding; instead, a complex function involving the orientation of the grain boundary and the orientation difference between the two grains gave a more exact measure of boundary sliding (6). These same relationships are being studied for fatigue (axial) loading conditions for 5 and 150 percent per minute strain rates.

Cracking appears to be initiated at grain boundaries, but failures are transgranular at temperatures up to about 600°F. At 600°F and higher, the fractures become intergranular. Of interest are grain and grain boundary orientations which initiate cracks and along which cracks are extended.

A large number of single crystal bars have been grown which are suitable for specimen machining and test. A number of tests have been completed but the amount of data is inadequate for interpretation. A complete temperature study of cycles to failure versus temperature is not planned since most of the testing will be of the interrupted variety. Most of the orientations of these single crystals are those with <110> or <111> directions parallel or nearly parallel to the specimen axis.

Discussion

Much of the discussion of this section is of a preliminary type since considerably more work needs to be done. The single crystal work has already shown that specimens with <110> parallel to the strain axis show markedly higher fatigue life than those with <111> . This is true both at room temperature and 800°F. This is probably due to the fact that of the orientations of the two sets of slip planes, the {111} is approximately 10° from the plane of maximum shear stress in the <110> crystal, whereas, in the <111> crystal, the three sets of {111} planes nearest the 45° direction are all about 25° away. Surface replicas after one cycle show this orientation effect quite plainly. For the <110> parallel to the specimen axis, the two intersecting slip planes are both seen to be at an angle of about 10° with the maximum shear stress direction. Further cycling shows rotation of {111} planes into the 45° direction. The smaller amounts of rotation necessary to bring the {111} planes in line with maximum shear stress for the <110> crystal leads to longer fatigue life before crack initiation. The large scale bending of the crystal with the <111> parallel to the strain axis, in the effort to rotate {111} planes 45° to the tensile axis, leads to earlier cracking than in the <110> crystal. The fatigue life of a <110> crystal at room temperature is ten times that of a <111> crystal. As temperature increases this difference decreases, becoming a factor of about two at 800°F.

It is interesting to note that X-ray orientation studies of coarse grained polycrystalline specimens show a similar effect. In the orientation analysis of abutting grains, for high temperature fatigue, where grain boundary movement is strongly concentrated in one of two grains, the grain which accommodates the movement seems to have {111} planes more favorably oriented to the maximum shear stress direction. Interrupted tests after several cycles show that strong grain boundary movement is also associated with large orientation differences between adjacent grains. Preliminary Laue-back-reflection studies for heavily migrated grain boundaries, after 1/2 cycle at 800°F, show that subgrain formation is present in both grains, but more abundant in one of the grains. At low temperatures the intense lattice bending at grain boundaries cannot be absorbed by a rearrangement of atoms to reduce strain, i.e., through polygonization, and therefore cracking results. Note in Figures 31 and 32 the severe lattice bending occurring on one side of a grain boundary in room temperature tests.

The micrographs in Figures 24, 26, 27, 28, 33, 34, all show extensive grain boundary movements, usually on one side of a boundary between adjacent grains. Figure 32 shows particularly well the nature of grain boundary movement. The faint slip traces show that slip first progressed up to the grain boundary, but the intense strain at the boundary led to shearing in the adjacent material; deformation bands and substructures are clearly apparent. The slip bands act as reference markers in such instances.

Representative views are shown in the following of typical and interesting structures.

Figure 24 shows grain boundary shear and migration after 8 cycles at 5 percent strain per minute at 800°F, using a surface replication method at a magnification of 900X.

Figure 25 shows coarse cross slip, grain boundary sliding and grain boundary migration after only 2 cycles at 5 percent strain per minute at 800°F, using surface replication at 100X. Note the extensive folds at three triple points. This is the prelude to extensive boundary migration which leads to grain boundary orientation of 45°.

Figure 26 shows, in addition to features found in Figure 25, subgrain formation and grain boundary serrations (8) after 1/2 cycle at 1.5 percent strain per minute at 800°F. This figure taken with a conventional light microscope may be compared to Figures 27 and 30, taken with an interference contrast microscope. Note the greater detail of surface markings in the latter pictures. In particular, due to small changes in orientation across a kink boundary, this method emphasizes the shadow effect more vividly (see especially Figure 29). Slip bands and subgrains are also sharply defined.

In general, it is noted that the higher strain rate of 150 percent per minute gives a smoother and more uniform surface than the 5 pereent rate (compare Figures 27 and 28).

Figures 31 to 34 show at fairly high magnification a number of interesting details of grain boundary shear and migration. In particular, Figures 31 and 32 have caused considerable speculation regarding the nature of grain boundary shear (6,9). In these two figures one observes somewhat more closely spaced slip bands (heavy) which are straight to the grain boundary; the opposite grain, with coarser slip bands, shows extensive bending. This suggests that the former grains slip, building up strain energy at the boundary interface. Two slip systems are required in the second grain to accommodate the imposed strain; this probably leads to deformation band formation, along with subgrain formation.

The very dark regions in Figure 31 may be due to artifacts in stripping the replica as a result of grain boundary cracking. It is clear that considerably more study and close follow-up of the deformation and fracture modes is required of the grain boundary.

Figures 35 to 40 are Laue back-reflection views across grain boundaries undergoing shear and migration at 800°F. Figure 35 is a pattern taken with the beam impinging on both grains across a grain boundary, prior to fatigue deformation. Figure 36 is nearly the same position after 2 percent compression in one-half cycle, at 800°F. Considerable subgrain formation has occurred, with small angular rotation; it is also obvious that enough migration has occurred that only the orientation of one grain is clearly recorded. Figures 37 to 40 show other views, taken in each grain, showing the inhomogeneous deformation, evident primarily via the subgrain formation route. As in creep, severe bending and crystal breakdown occur near the grain boundary and the degree of breakdown is always more severe in one grain than in the other (2,4), confirming the structures observed in Figures 31 and 32.

Overall, it appears that if strain rate and temperature conditions are similar, low cycle fatigue yields similar patterns of deformation and fracture as are observed in axial creep. The severity of deformation, the rates of grain boundary migration, the increased tendency for kinking, and other features are different in degree rather than in kind. Much less can be said regarding fracture mechanics at this stage. The unusual migration of grain boundaries to 45° positions is an entirely new observation. Additional studies should provide answers to the questions which have been raised.

CONCLUSIONS

It was the purpose of this program to examine the effects of strain rate on fatigue behavior. As such, low strain rates were necessary to permit grain boundary sliding and migration, along with other common modes of deformation. The other important variables were temperature, grain size, and composition.

The conclusions are based on an essentially constant strain rate, axially loaded test.

1. At strain rates of 5 and 150 percent per minute, at a strain amplitude of $\pm$ 1 percent, strain rate effects are observed above 500°F. Increasing strain rate results in an increase in cycles to failure up to about 700 or 800°F.

2. Increasing the test temperature increases the cycles to failure up to 600 or 800°F, depending on strain rate and grain size.

3. Both pure aluminum and an aluminum - 10 percent zinc alloy show higher cycles to failure for the coarse grained compared to fine grained condition from 80 to 500°F. This is an unexpected and unexplained behavior.

4. Aluminum of greater than 99.995 percent purity has never been observed to show intergranular cracks in an air atmosphere, regardless of strain rate or temperature; accordingly intergranular cracking at 80°F must be classed as unusual.

5. Above 700°F, high purity aluminum undergoes extensive grain boundary migration with triple points following deformation folds to form 45° grain boundary intersections (including an unstable configuration of surface quadruple points). Boundary shear becomes easy with extensive intergranular cracking.

6. Associated with intercrystalline cracking of pure aluminum above 700°F is copious void formation along the 45° grain boundaries. In creep, such voids are never observed in high purity aluminum, regardless of temperature or strain rate.

7. The aluminum - 10 percent zinc alloy behaves similarly in almost all respects to high purity aluminum above about 500°F. At 80°F severe intergranular cracking takes place, with resultant poor life. The unequal strengthening of grains and grain boundaries leads to relative grain boundary weakness and embrittlement. Some grain boundary shear actually takes place at 80°F.

REFERENCES

1. I. S. Servi and N. J. Grant: Trans. AIME, J. Metals, 3, October 1951, p. 909.
2. H. C. Chang and N. J. Grant: Trans. AIME J. Metals, 4, June 1952, p. 619.
3. H. C. Chang and N. J. Grant: Trans. AIME, J. Metals, 5, February 1953, p. 305.
4. A. M. Gervais, J. T. Norton, and N. J. Grant: Trans. AIME, J. Metals, 5, September 1953, p. 1166.
5. H. C. Chang and N. J. Grant: Trans. AIME, J. Metals, 8, May 1956, p. 544.
6. A. W. Mullendore and N. J. Grant: Trans. AIME Met. Soc. 227, April 1963, p. 319.
7. H. Brunner and N. J. Grant: Trans. AIME, 218, February 1960, p. 122.
8. A. W. Mullendore and N. J. Grant: (Chapter) Structural Processes in Creep, Special Report No. 70, The Iron and Steel Institute, London, 1961.
9. F. N. Rhines, W. E. Bond, and M. A. Kissel: Trans. ASM, 48, 1956, p. 919.

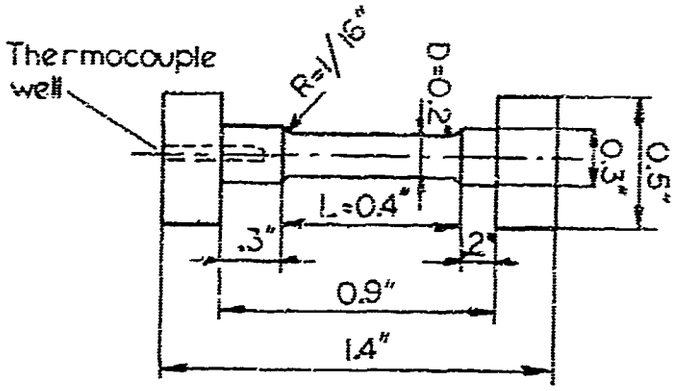

Figure 1. Dimensions of the low cycle fatigue specimens.

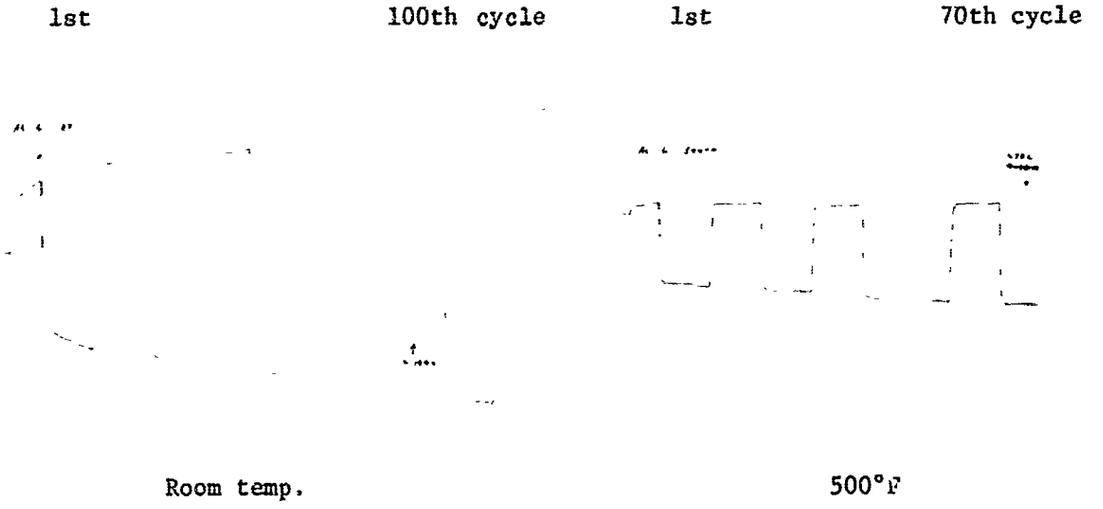

Figure 2. Load vs. elapsed time of individual cycles curves for coarse grained 99.99% aluminum specimens tested at room temperature and at 500°F. Strain rate 5% per minute. Strain amplitude 2%.

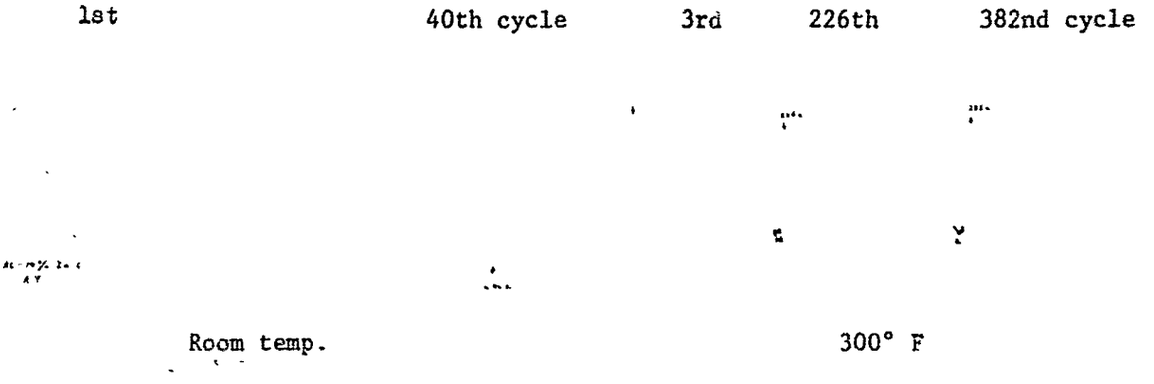

Figure 3. Load vs. elapsed time of individual cycles curves for coarse grained aluminum - 10% zinc specimens tested at room temperature and at 300°F. Strain rate 5% per minute. Strain amplitude 2%.

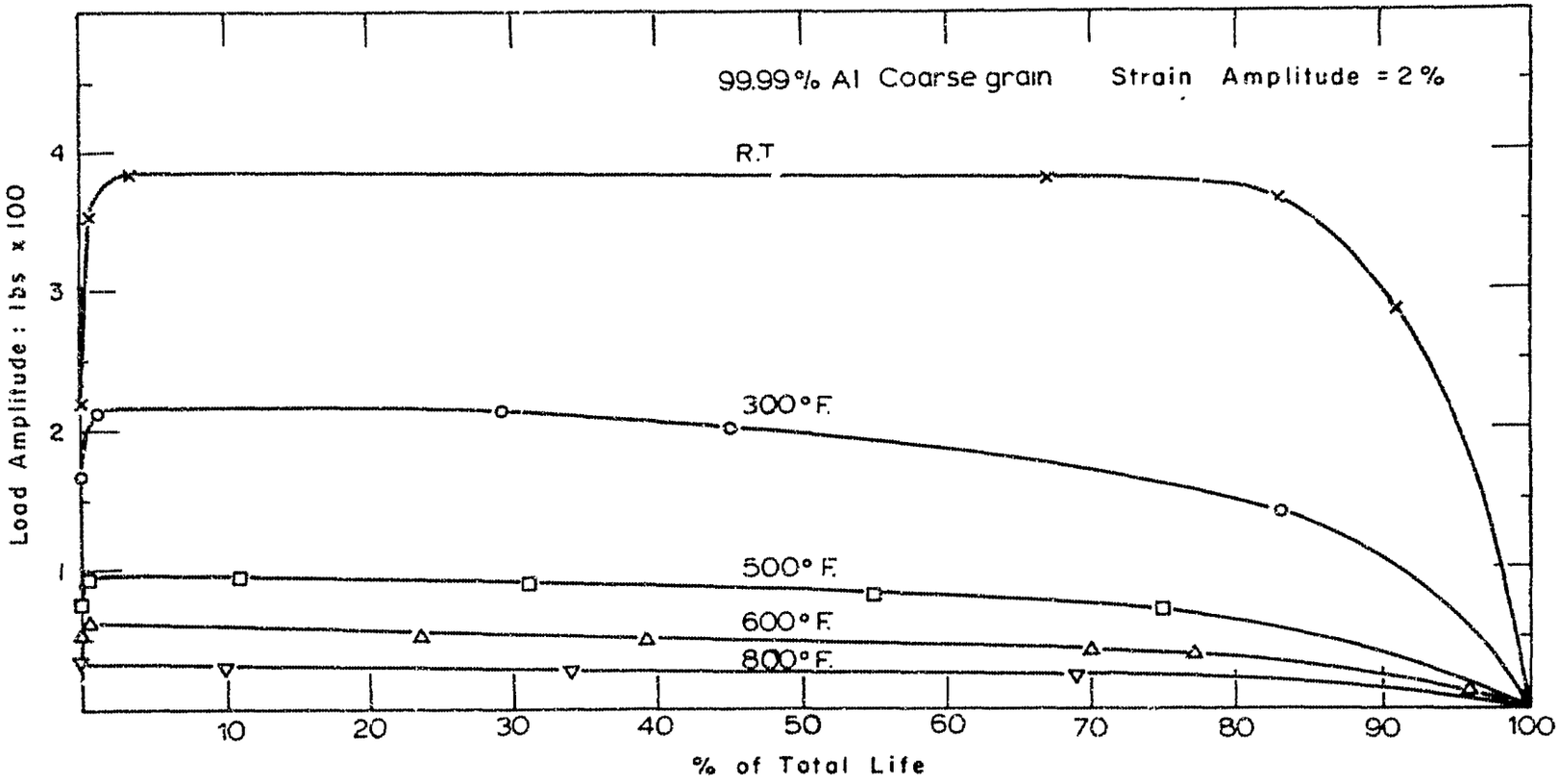

Figure 4. Load amplitude vs. percent of total specimen life at different temperatures for 99.99+% aluminum. Coarse grained specimens.

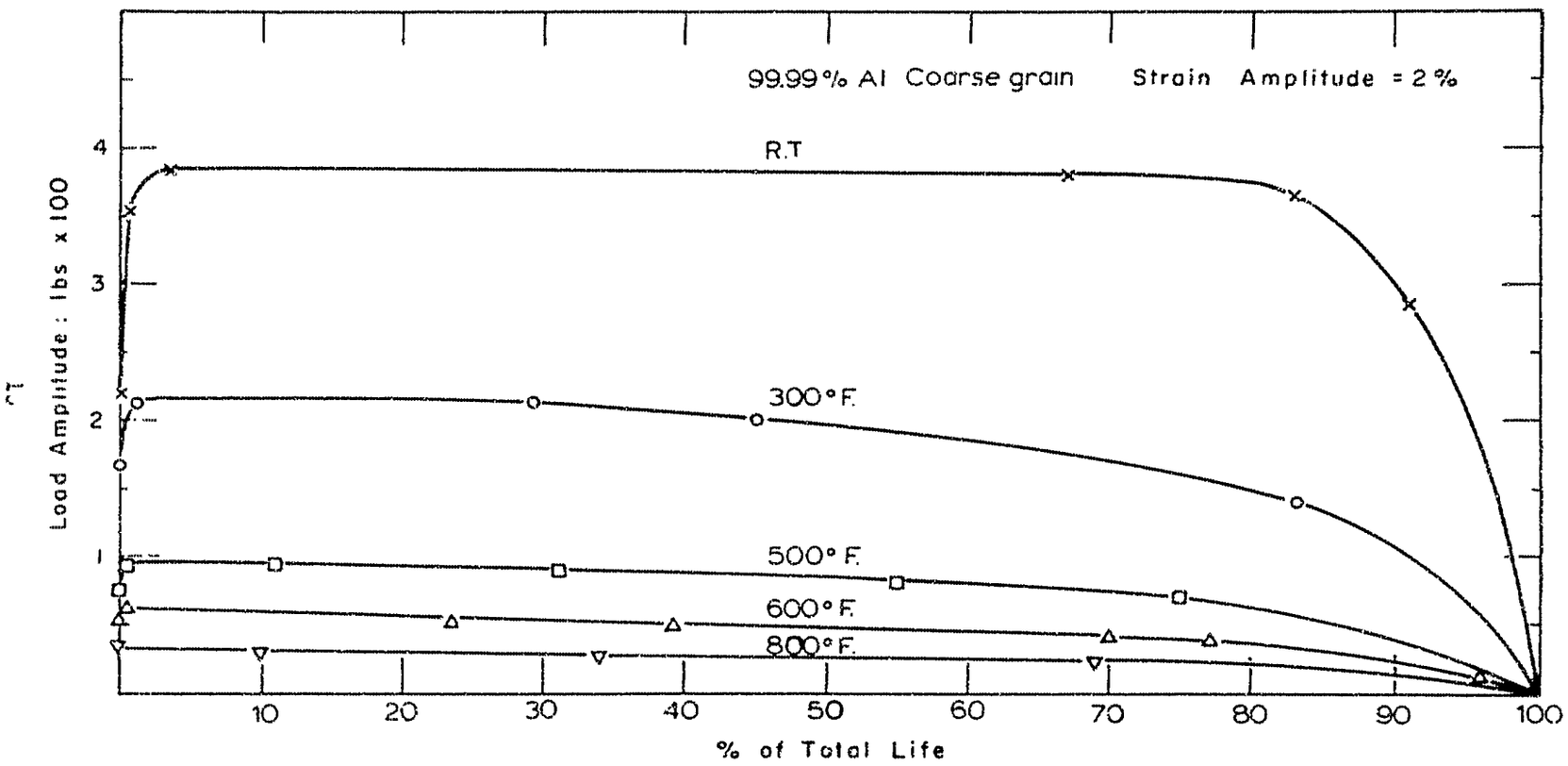

Figure 5. Load amplitude vs. percent of total specimen life at different temperatures for aluminum - 10% zinc. Coarse grained specimens.

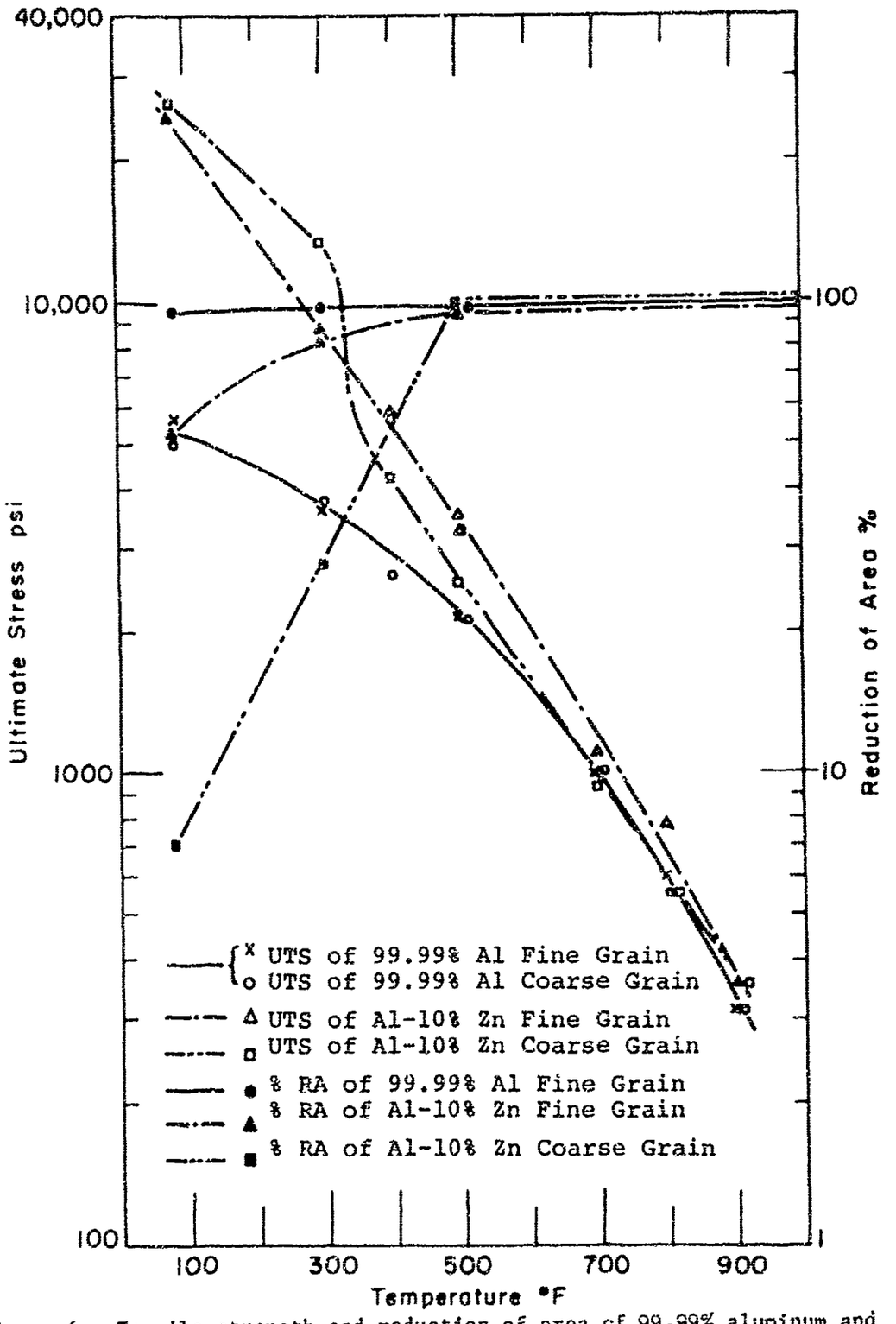

Figure 6. Tensile strength and reduction of area of 99.99% aluminum and aluminum - 10% zinc in the function of temperature.

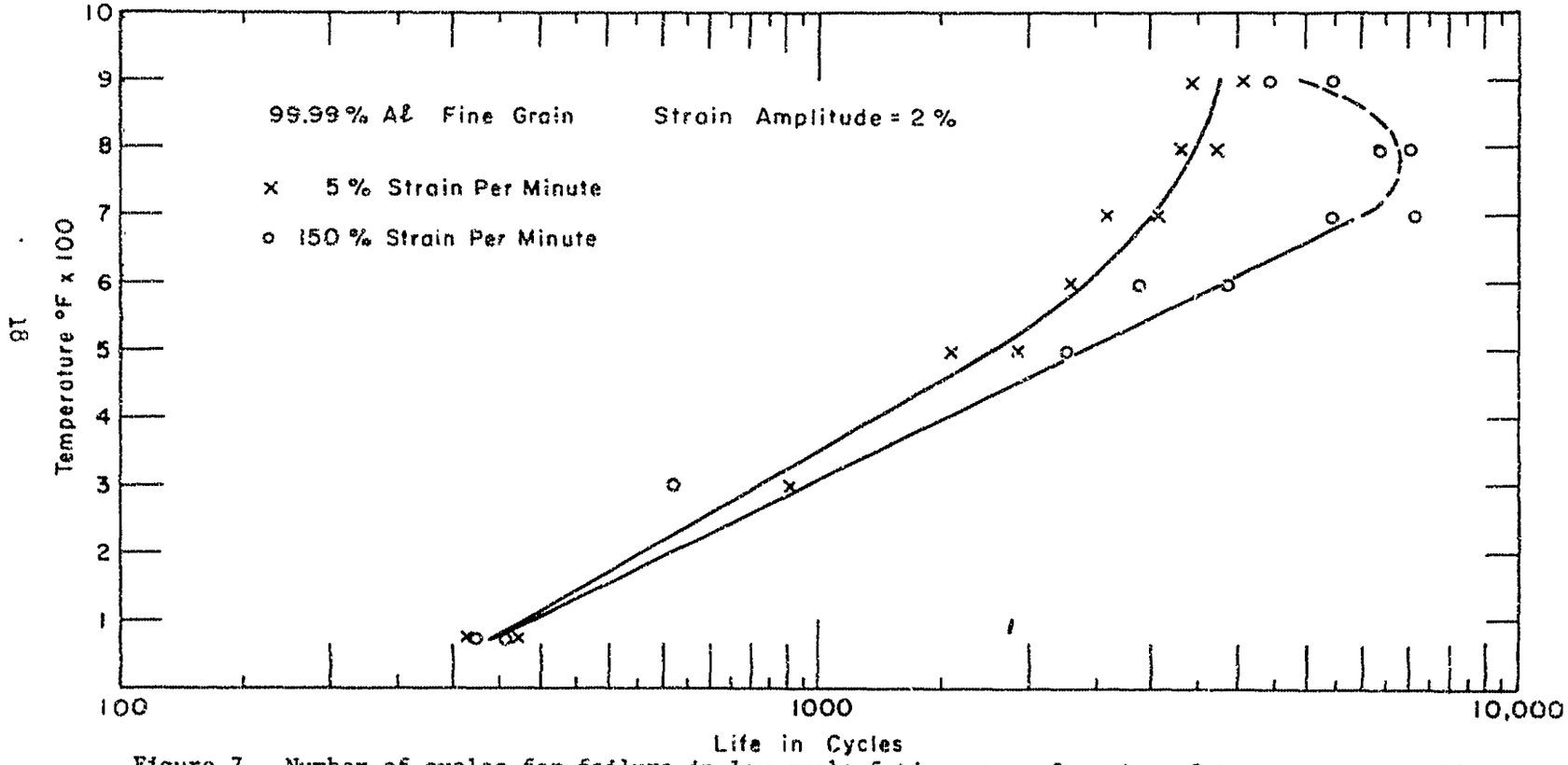

Figure 7. Number of cycles for failure in low cycle fatigue as a function of temperature for fine grained 99.99% aluminum.

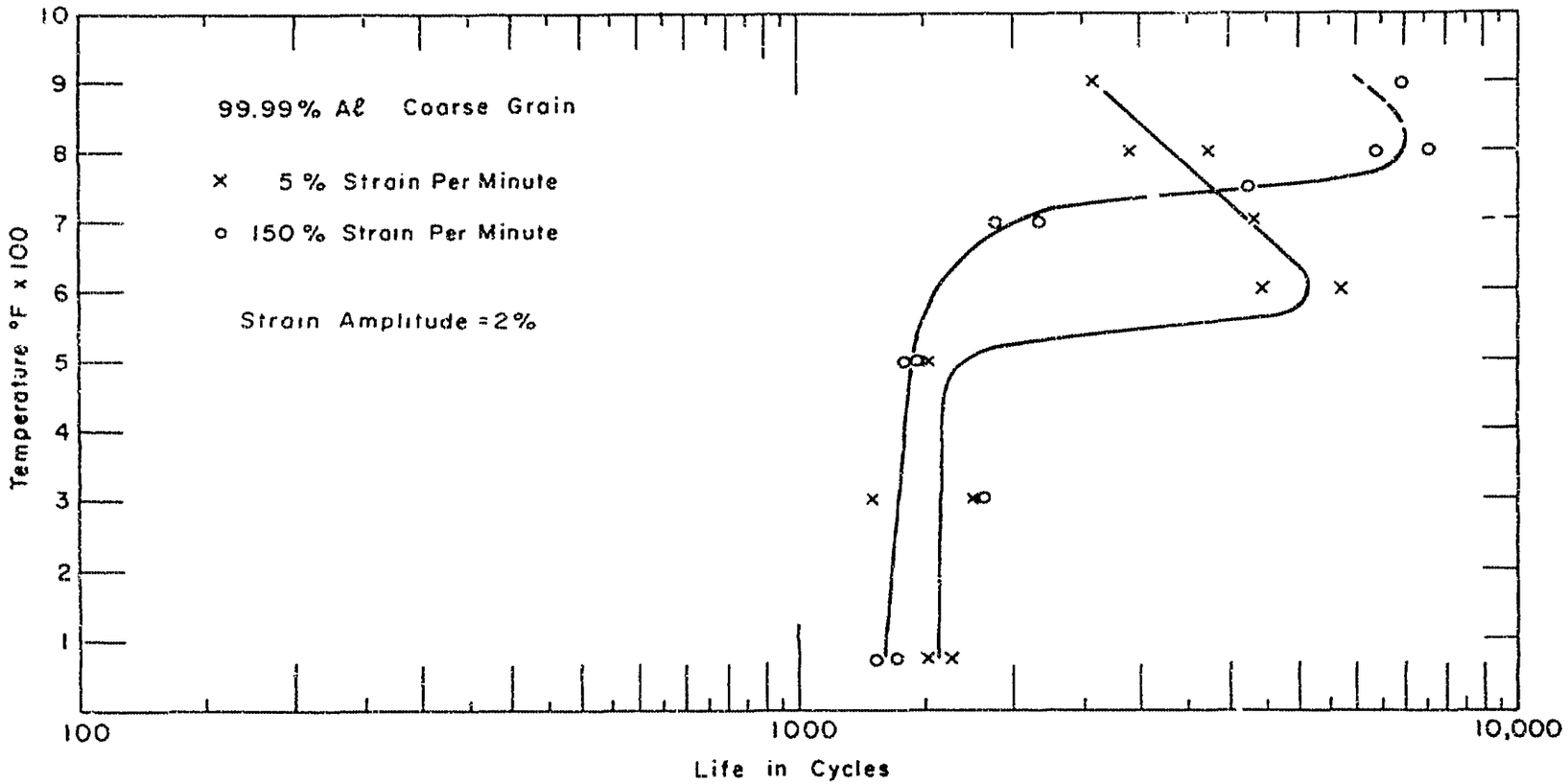

Figure 8. Number of cycles for failure in low cycle fatigue as a function of temperature for coarse grained 99.99 % aluminum.

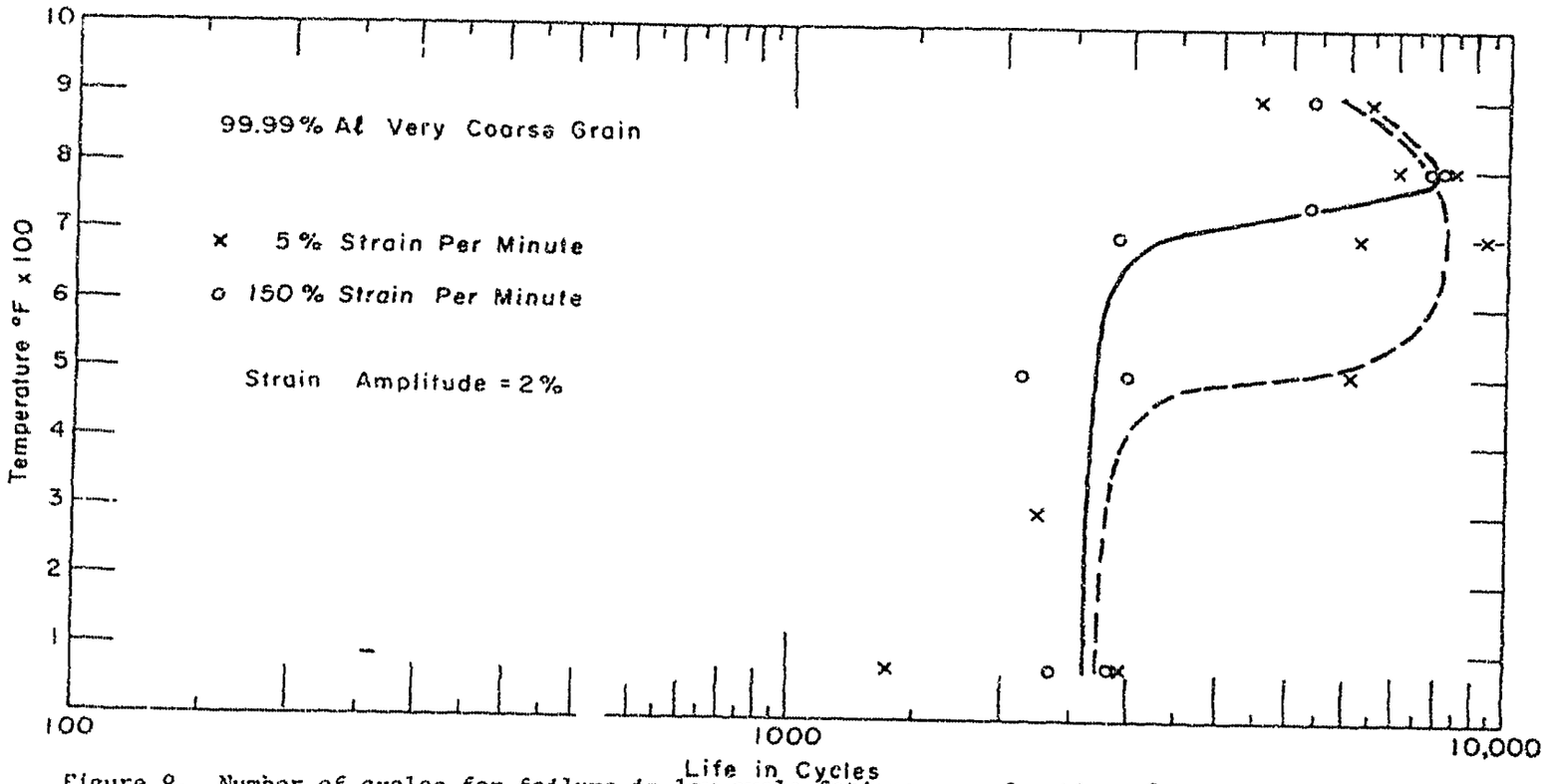

Figure 9. Number of cycles for failure in low cycle fatigue as a function of temperature for very coarse grained 99.99% aluminum.

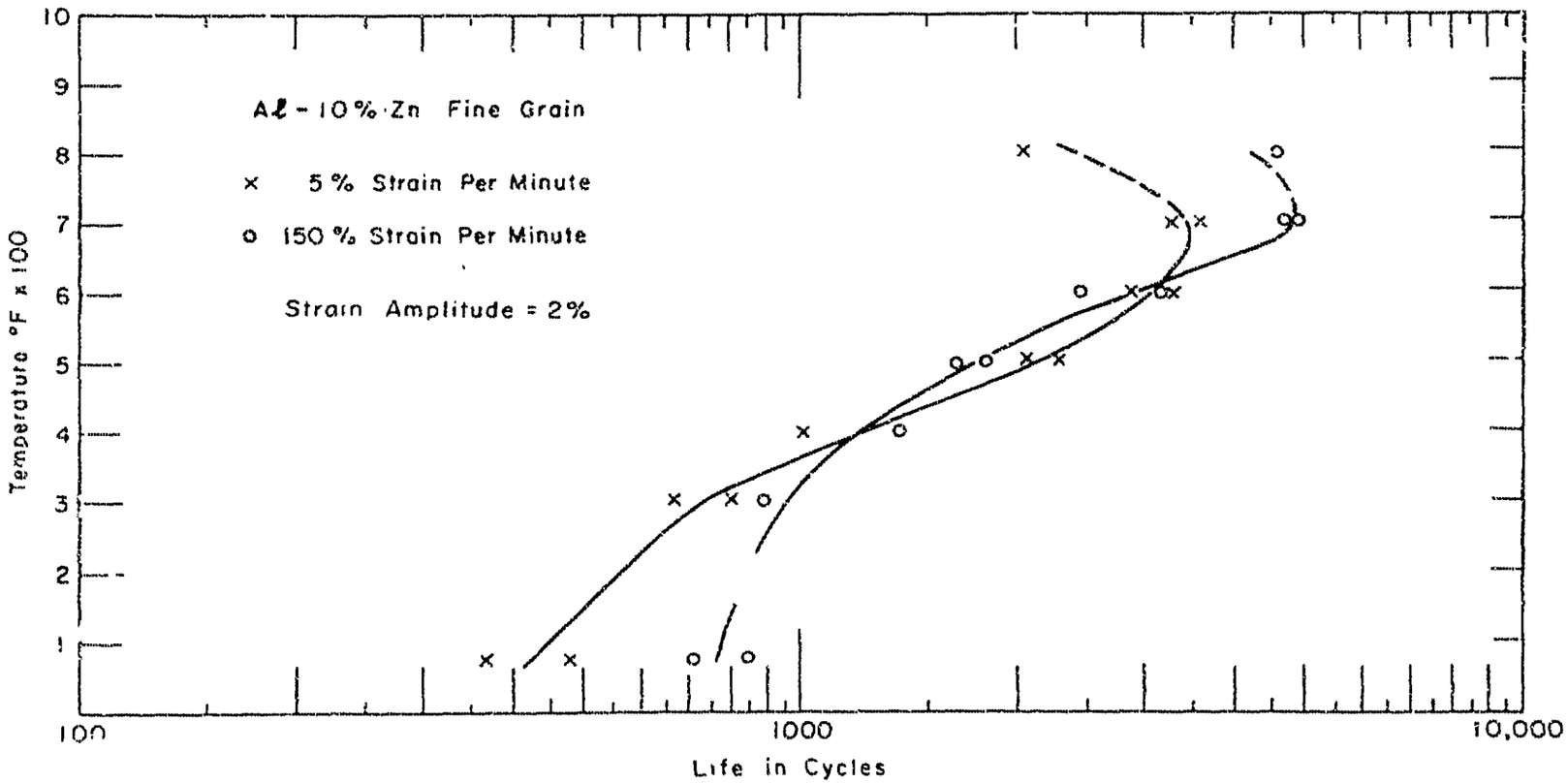

Figure 10. Number of cycles for failure in low cycle fatigue as a function of temperature for fine grained aluminum - 10 percent zinc.

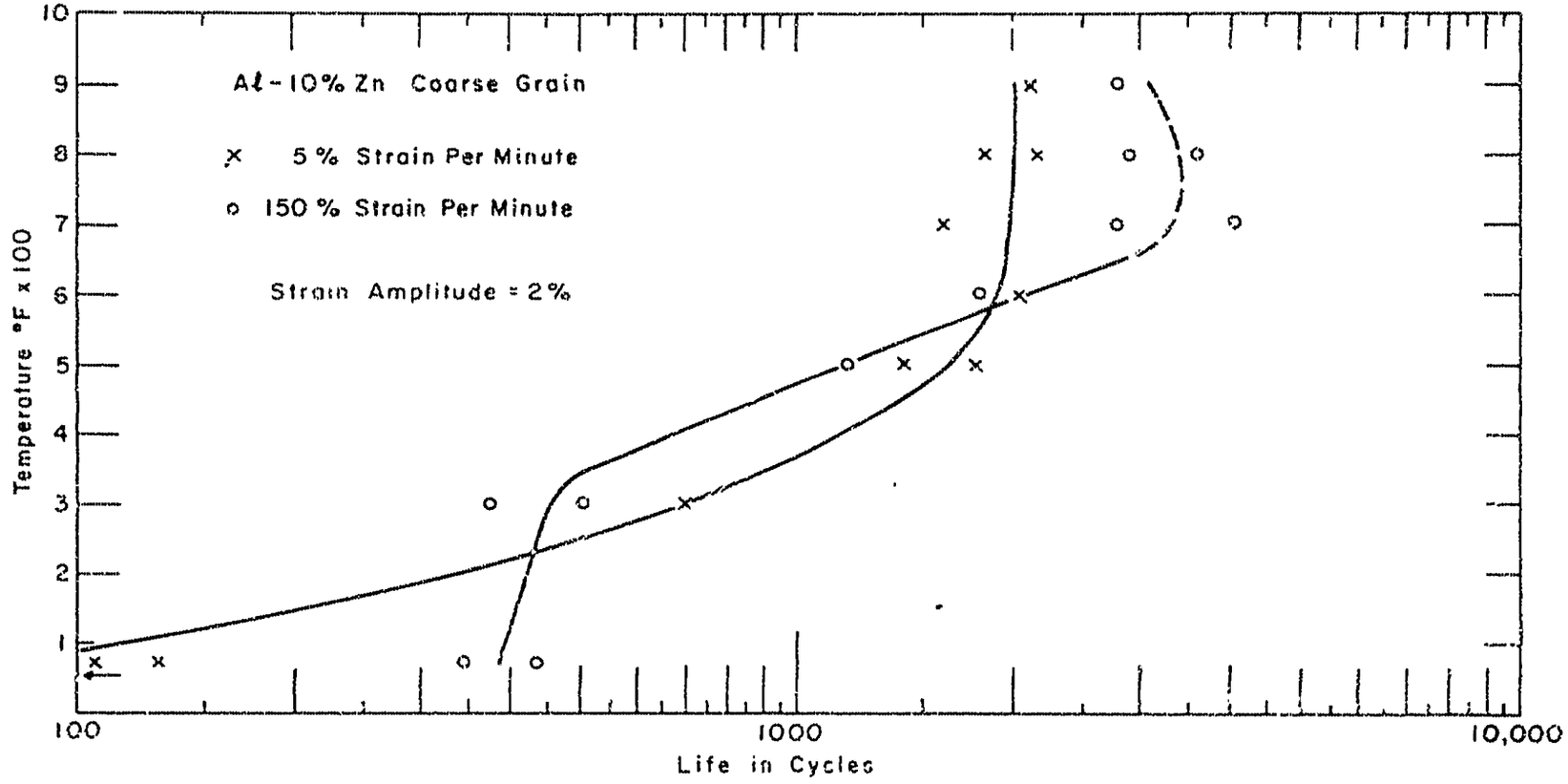

Figure 11. Number of cycles for failure in low cycle fatigue as a function of temperature for coarse grained aluminum - 10 percent zinc.

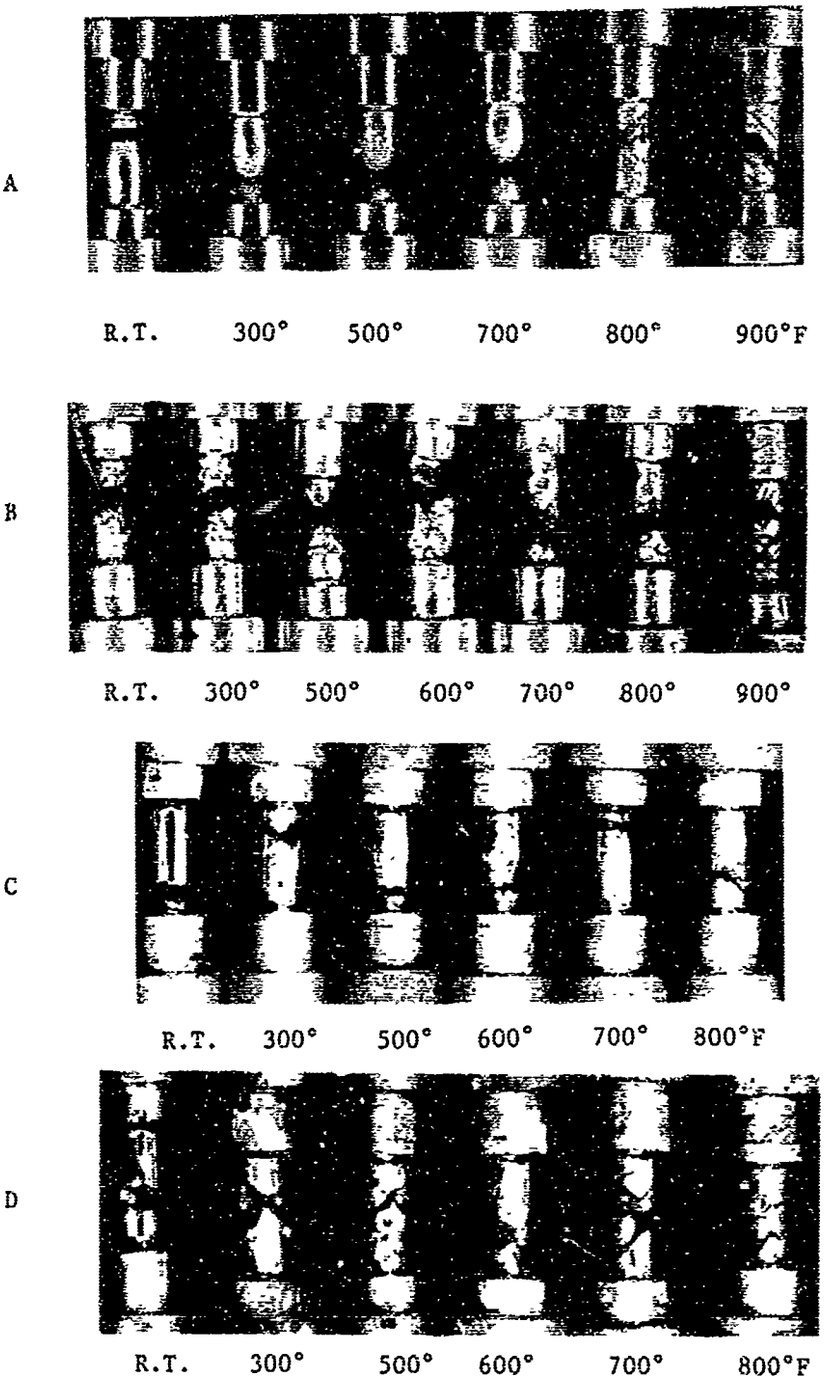

Figure 12. 99.9 . Al and Al - 10% Zn specimens tested to failure in low cycle fatigue at different temperatures. Strain rate 5% per minute; strain amplitude 2%.

A. Fine grained pure aluminum
B. Coarse grained pure aluminum
C. Fine grained Al -10% Zn alloy
D. Coarse grained Al - 10% Zn alloy

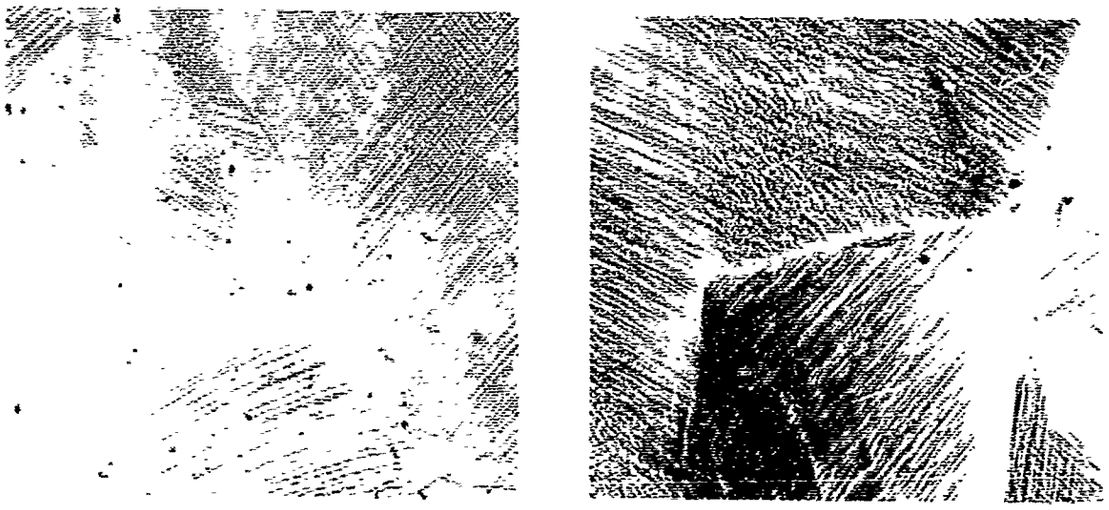

A B

C

Figure 13. Surface deformation in coarse grained 99.99% Al interrupted after increasing cycles at room temperature.
A. After 1/2; B. After 10; C. After 100 cycles. 50X.

A

B

Figure 14. Surface deformation in coarse grained 99.99% aluminum tested for 10 cycles at 600°F, at 5 and 150% per minute strain rates. A. At 150% per minute; B. At 5% per minute. 50X.

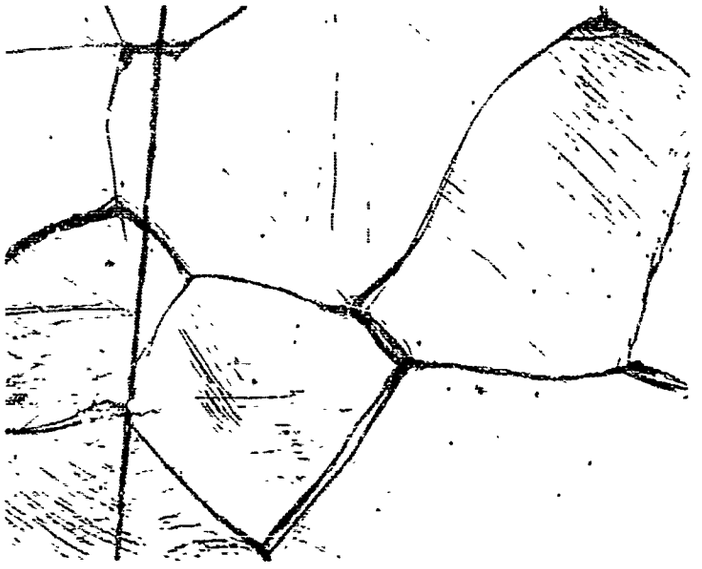

A

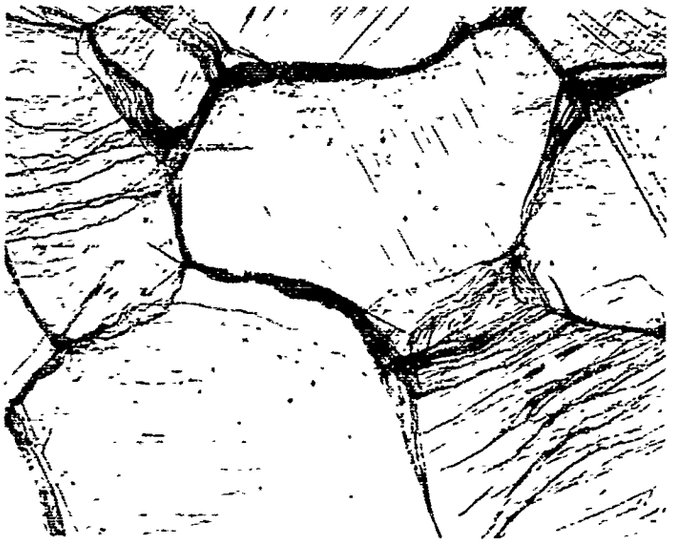

B

Figure 15. Surface deformation in coarse grained 99.99% aluminum tested for 10 cycles at 800°F, at 5 and 150% per minute strain rates. A. At 150% per minute; B. At 5% per minute. 50X.

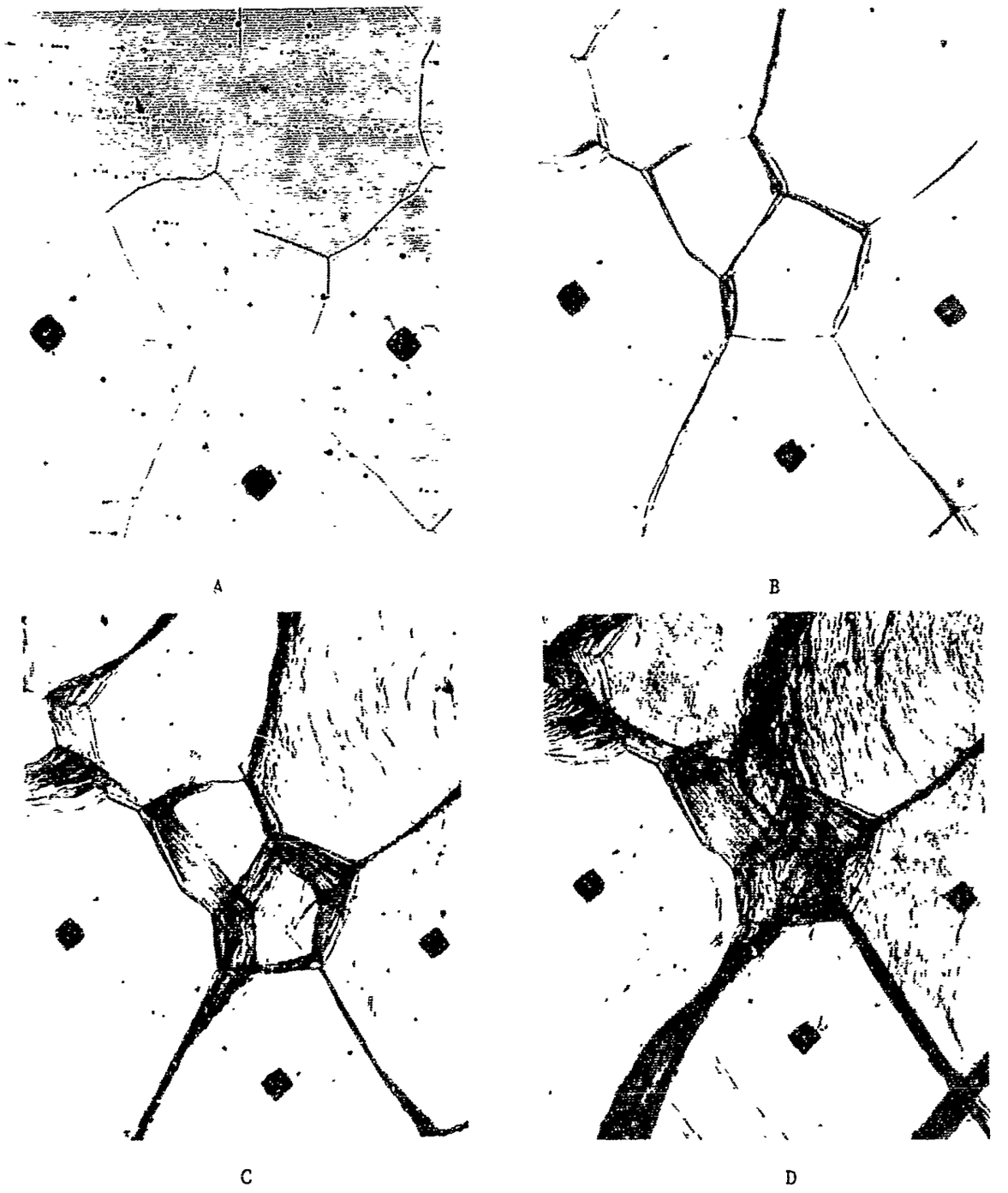

Figure 16. Surface markings in fatigued coarse grained aluminum at 800°F for a strain rate of 5% per minute. 50X.
A. Before testing
B. After 2 cycles
C. After 20 cycles
D. After 100 cycles

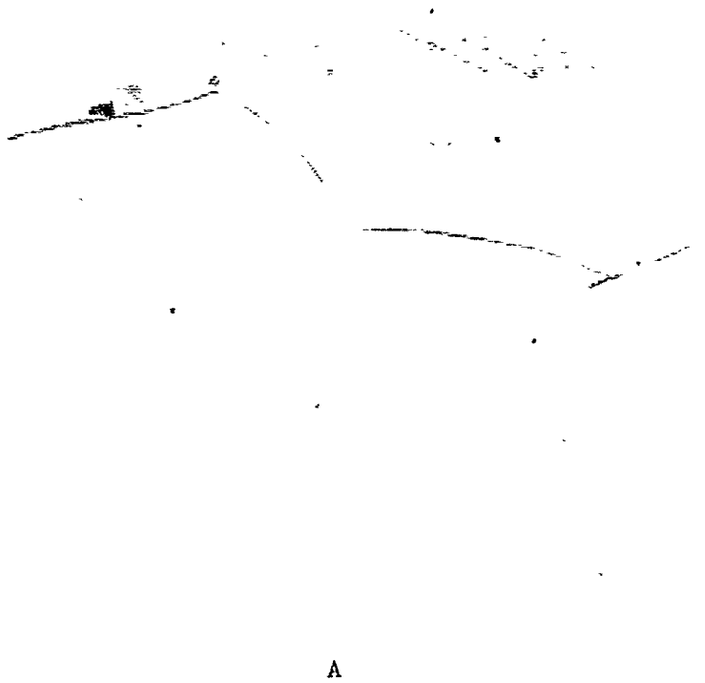

A

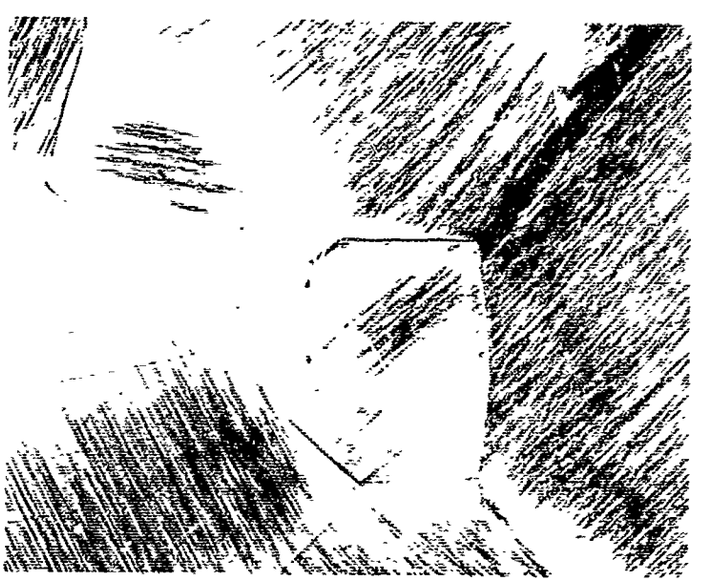

B

Figure 17. Surface deformation of coarse grained aluminum - 10% zinc tested at 80 and 300°F at a strain rate of 5% per minute. 50X.
A. After 10 cycles at 80°F
B. After 10 cycles at 300°.

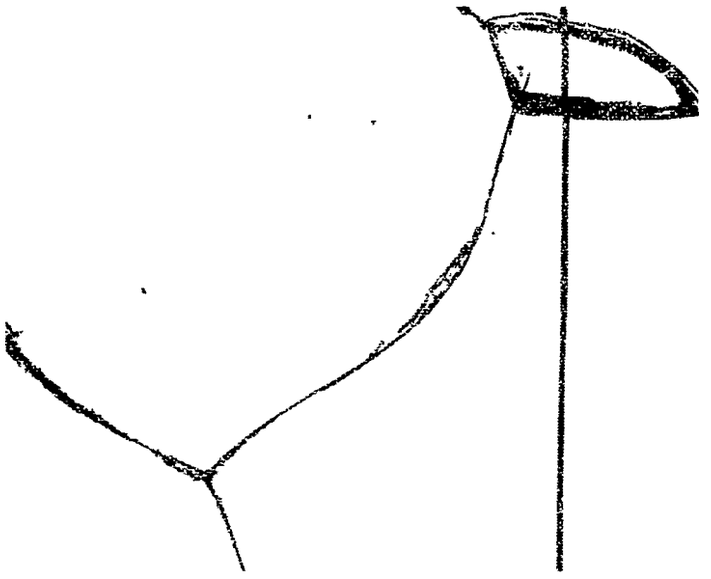

C

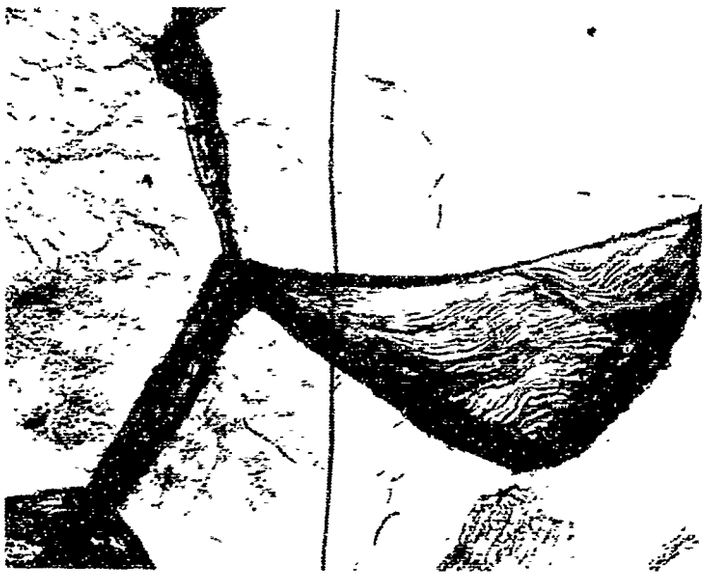

D

Figure 17 (continued) 50X

C. After 10 cycles at 700°F
D. After 100 cycles at 800°F.

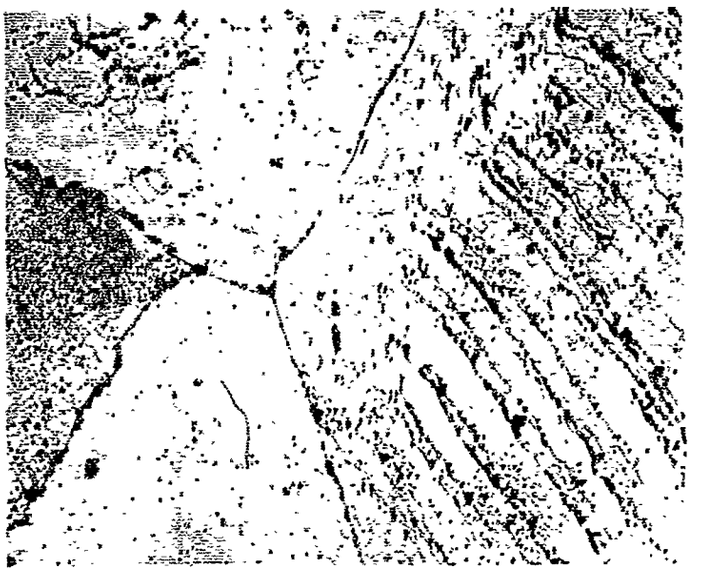

Figure 18. Subgrain formation along slip bands in 99.99% aluminum tested at room temperature for 1000 cycles. Note also the fine subgrain structure. 250X.

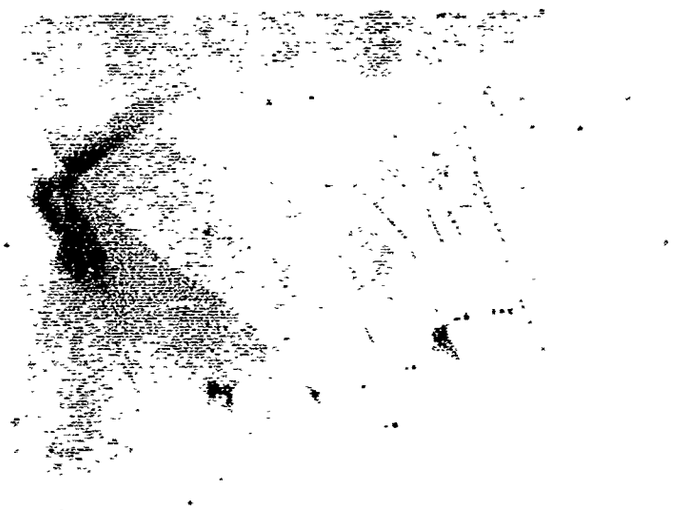

Figure 19. Microcrack formation along slip planes in 99.99% aluminum tested for 1000 cycles at 600°F at 5% strain per minute. Etched with 0.5% HF_2. 250X.

A

B

Figure 20. Microstructure of fine grained 99.99% aluminum at the fracture ter testing at a strain rate of 5% per minute. Specimen axis was h ntal. 50X.
A. Tested at 700°F; B. Tested at 800°F.

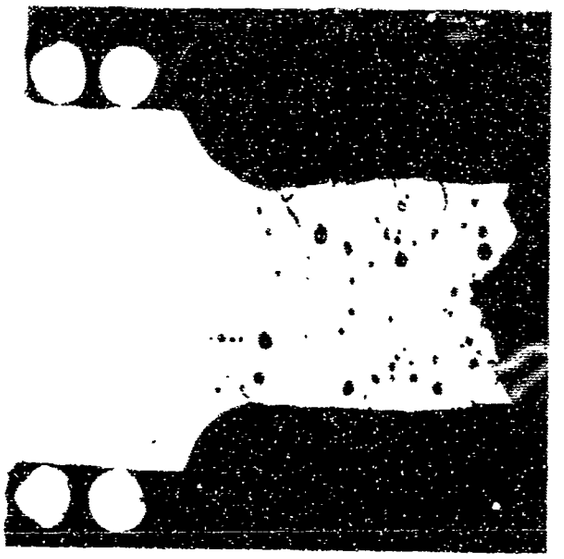

Figure 21. Void formation and intergranular cracking in fine grained aluminum-10% zinc tested at 700°F at 5% strain per minute. Electropolished, unetched. Approximately 12X.

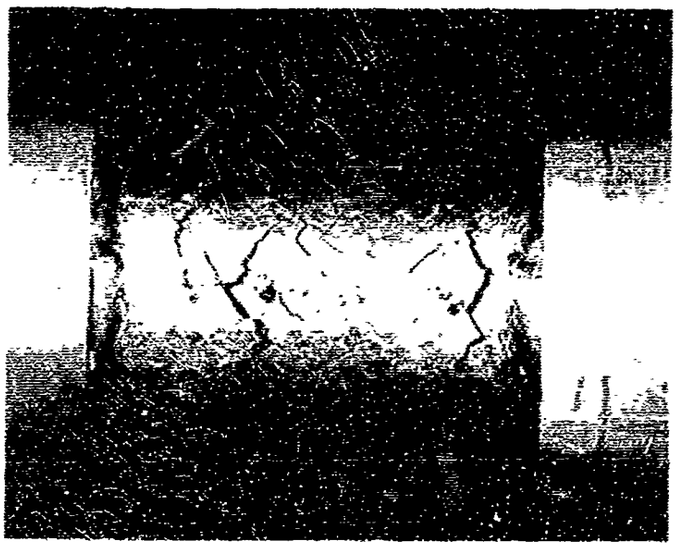

Figure 22. Intergranular cracking inward from the free surface of fine grained aluminum - 10% zinc along migrated 45° grain boundaries. The specimen was tested for 1500 cycles at 800°F at 5% strain per minute. Approximately 12X.

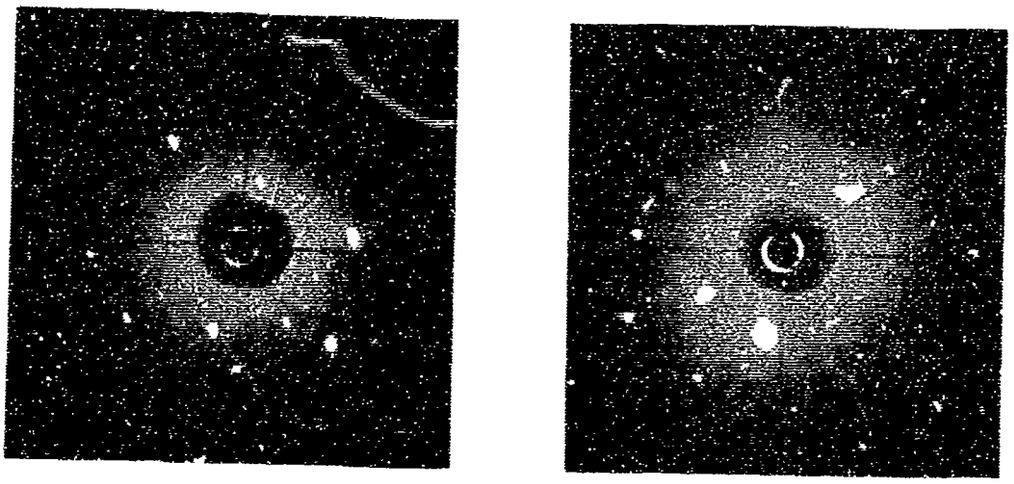

A B

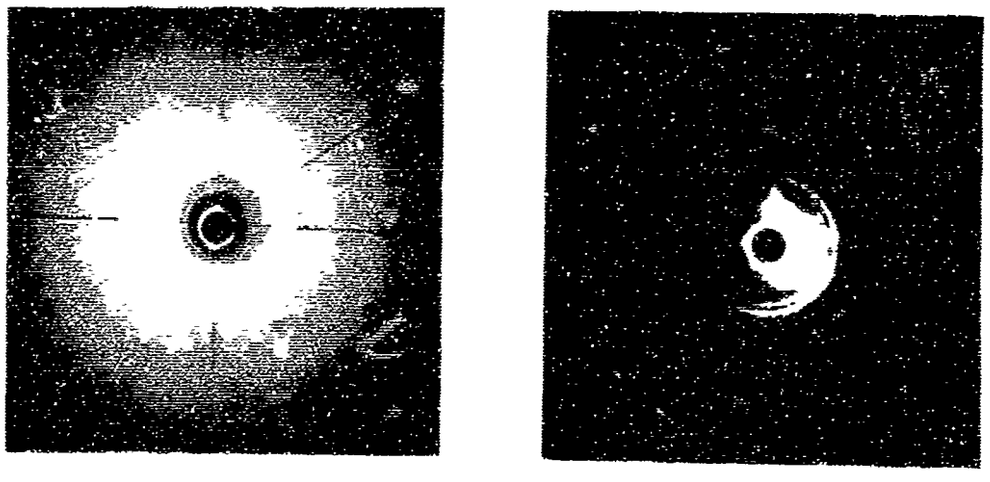

C D

Figure 23. Laue back-reflection pictures of coarse grained aluminum - 10% zinc and 99.99% aluminum specimens, tested in fatigue at room temperature at a strain rate of 5%/minute. Ni filtered Cu radiation.
A. Al - 10% Zn before testing
B. Al - 10% Zn after 130 cycles (tested to failure)
C. 99.99% Al before testing
D. 99.99% Al after 150 cycles

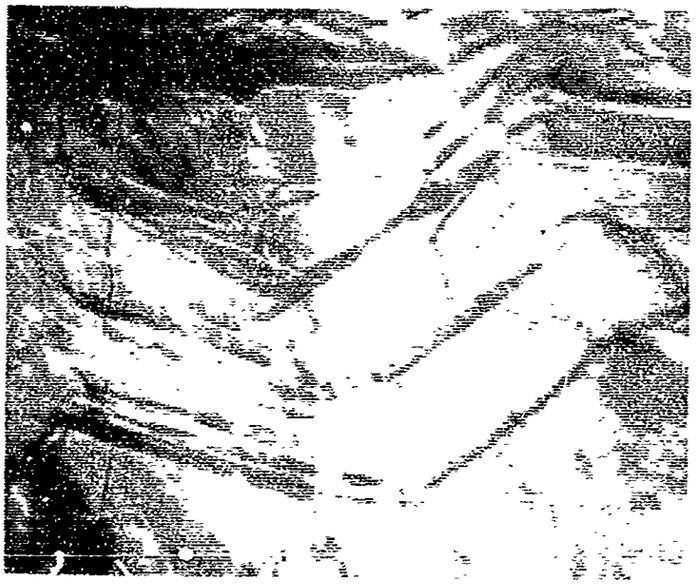

Figure 24. Sheared appearance of boundary movement after 8 cycles, ± 1 1/2% strain at 800°F. Surface replication method. 900X.

Figure 25. Boundaries tending to line up 45° to the strain axis (vertical) by fold formation and grain boundary migration. After 2 cycles, ± 1 1/2% strain at 800°F. Surface replication method. 100X.

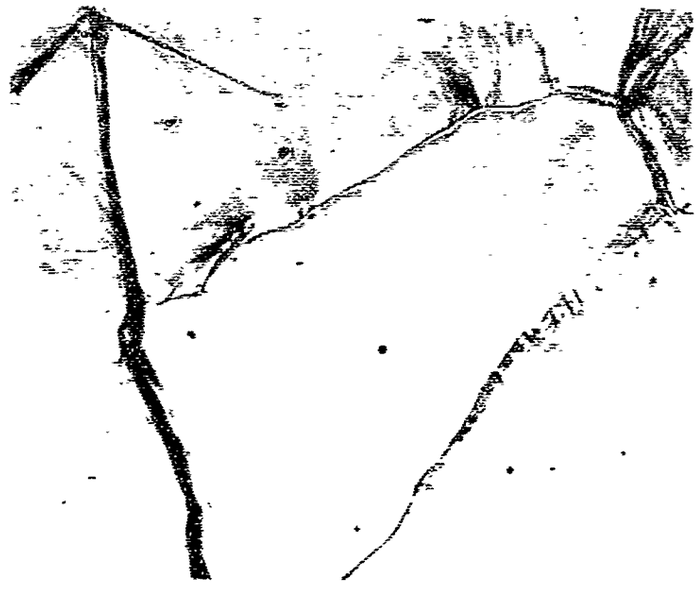

Figure 26. Grain boundary shear and migration leading to serrations in boundary and subgrain formation. After 1/2 cycle, ± 1 1/2% strain at 800°F. Surface replication method. 100X.

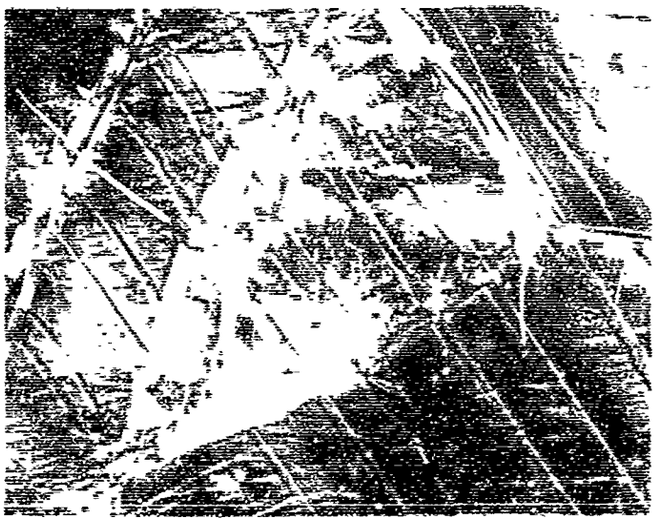

Figure 27. Grain boundary movements and other deformation at high strain rate (150%/minute). After 1 cycle, ± 2% strain, at 800°F. Surface replication method. Interference contrast. 100X.

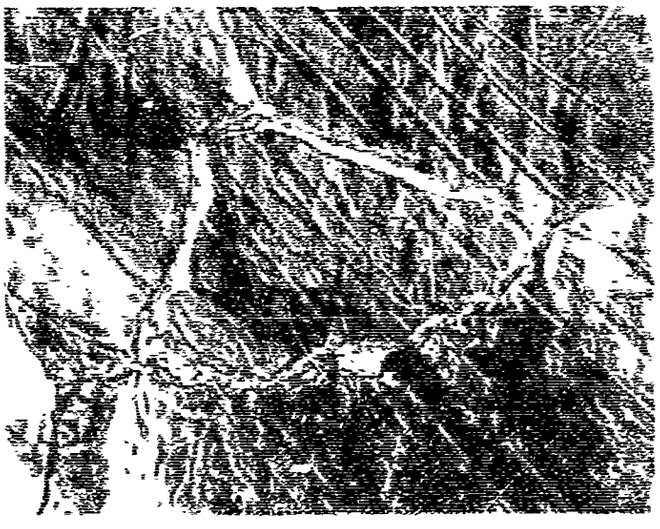

Figure 28. Grain boundary movements and other deformation at slow strain rate (5%/minute). After 1 cycle, ± 2% strain, at 800°F. Surface replication method. Interference contrast. 100X.

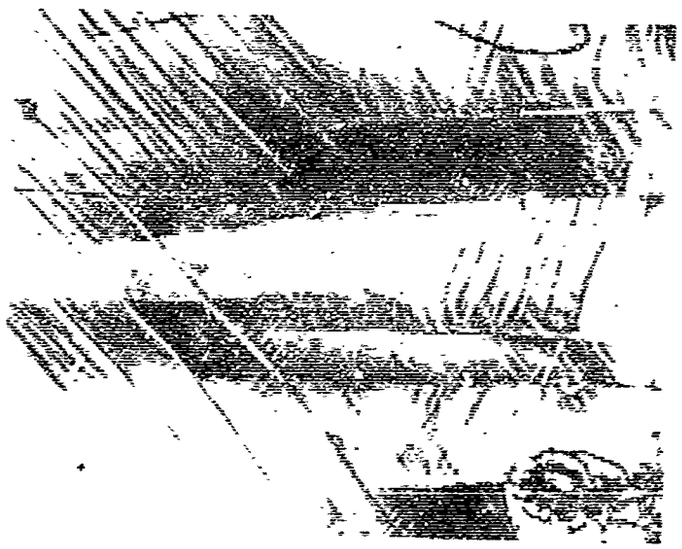

Figure 29. Kinking at high strain rate (150%/minute). After 1 cycle, $\pm$ 2% strain at 800°F. Surface replication method. Interference contrast. 100X.

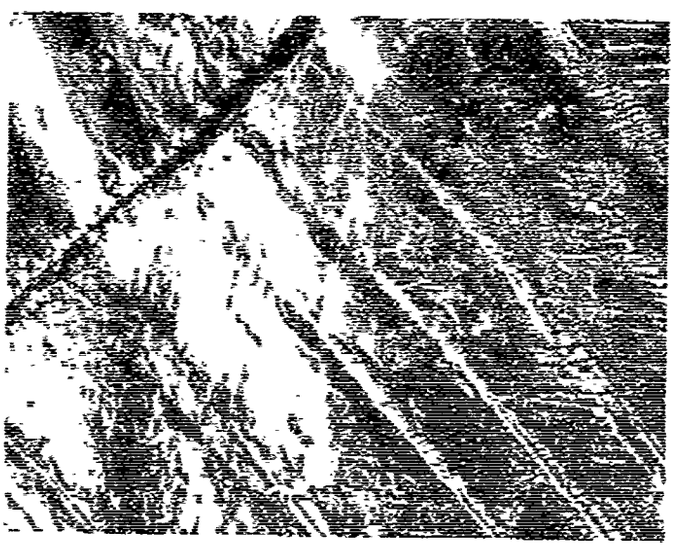

Figure 30. Kinking at low strain rate (5%/minute). After 1 cycle, $\pm$ 2% strain at 800°F. Surface replication method. Interference contrast. 100X.

Figure 31. Lattice bending adjacent to a grain boundary. After 50 cycles $\pm$ 1% strain at 80°F. Replication technique. Electron micrograph. 3000X.

Figure 32. Lattice bending adjacent to a grain boundary. After 50 cycles, $\pm$ 1% strain at 80°F. Replication technique. Electron micrograph. 2500X.

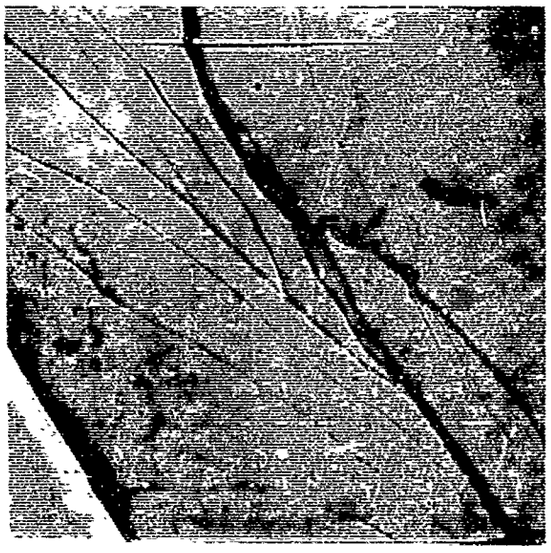

Figure 33. Grain boundary shear and migration adjacent to, and on one side of, original grain boundary at lower left. After 15 cycles, ± 1% strain at 650°F. Replication technique. Electron micrograph. 2500X.

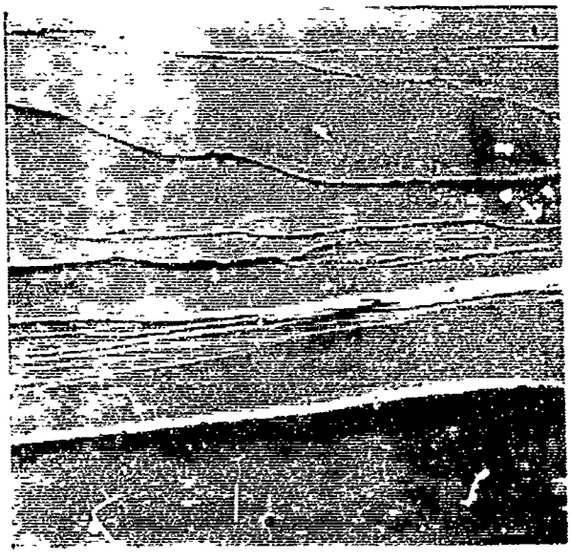

Figure 34. Grain boundary shear and migration adjacent to, and on one side of, original grain boundary near bottom. After 15 cycles, ± 1% strain at 650°F. Replication technique. Electron micrograph. 1500X.

Figure 35. Laue back-reflection pattern straddling grain boundary between grain (a) and grain (b). Before testing.

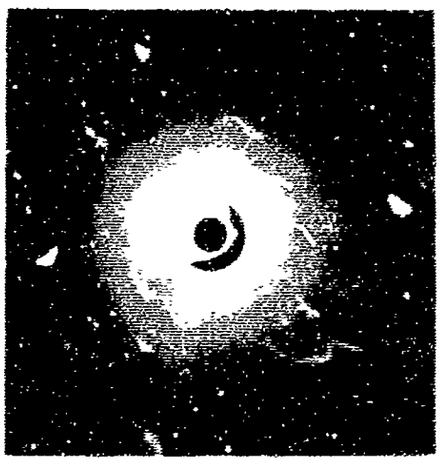

Figure 36. Same boundary as in Figure 35. After 2% compression at 800°F.

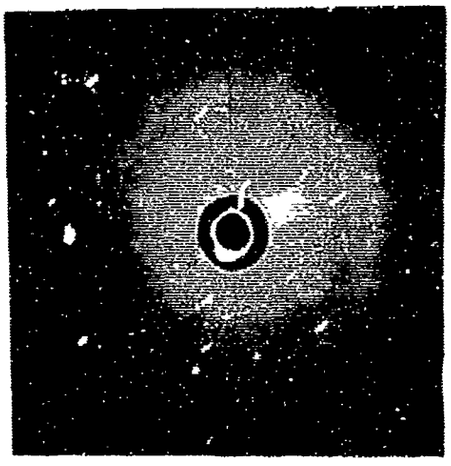

Figure 37. Area immediately adjacent to boundary of Figure 36. In grain (b). After 2% compression at 800°F. Fine collimator.

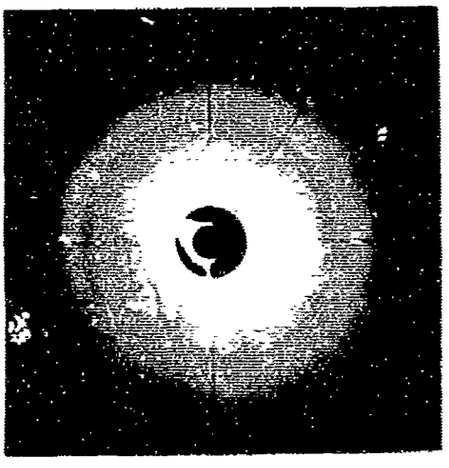

Figure 38. Area immediately adjacent to boundary of Figure 36. In grain (a). After 2% compression at 800°F. Fine collimator.

Figure 39. Area removed from boundary of Figure 36. In grain (b). After 2% compression at 800°F.

Figure 40. Area removed from boundary of Figure 36. In grain (a). After 2% compression at 800°F.

UNCLASSIFIED
Security Classification

DOCUMENT CONTROL DATA - R&D

(Security classification of title, body of abstract and indexing annotation must be entered when the overall report is classified)

1. ORIGINATING ACTIVITY (Corporate author) Massachusetts Institute of Technology Cambridge, Massachusetts	2a. REPORT SECURITY CLASSIFICATION UNCLASSIFIED 2b. GROUP

3. REPORT TITLE

RESEARCH ON THE ROLE OF STRAIN RATE AND TEMPERATURE IN FATIGUE

4. DESCRIPTIVE NOTES (Type of report and inclusive dates)

Summary Report - 1 November 1963 - September 1965

5. AUTHOR(S) (Last name, first name, initial)

Grant, Nicholas J., Blucher, Joseph, and Ritter, Donald L.

6. REPORT DATE	7a. TOTAL NO. OF PAGES	7b. NO. OF REFS
January 1967	41	9

8a. CONTRACT OR GRANT NO. AF 33(615)-1143 b. PROJECT NO. 7351 c. TASK NO. 735106 d.	9a. ORIGINATOR'S REPORT NUMBER(S) AFML-TR-66-39 9b. OTHER REPORT NO(S) (Any other numbers that may be assigned this report)

10 AVAILABILITY/LIMITATION NOTICES This document is subject to special export controls and each transmittal to foreign governments or foreign nationals may be made only with prior approval of the Metals and Ceramics Division (MAM), Air Force Materials Laboratory, Wright-Patterson AFB, Ohio.

11. SUPPLEMENTARY NOTES	12. SPONSORING MILITARY ACTIVITY Metals and Ceramics Division Air Force Materials Laboratory Wright-Patterson AFB, Ohio 45433

13. ABSTRACT

This study is concerned with the roles of strain rate and temperature on fatigue behavior. For the purposes of the immediate work pure aluminum and an aluminum - 10 percent zinc alloy were selected. To simplify analyses of the observed behavior, an axial fatigue machine was designed to eliminate strain rate and stress gradients in the specimen cross-section. Strain rates of 5 and 150 percent per minute, strains of ± 1 percent, and temperatures from 80 to 900°F were the variables studied. A number of grain sizes were utilized to evaluate the role of alloy structure. Other strain rates, strains and structures, including two phase systems, are being examined to extend the studies. Thermal fatigue behavior will be examined and the results compared with the present observations in mechanical fatigue.

DD FORM 1 JAN 64 1473

UNCLASSIFIED
Security Classification

Security Classification

14. KEY WORDS	LINK A		LINK B		LINK C	
	ROLE	WT	ROLE	WT	ROLE	WT
99.99% Pure Aluminum Al - 10% Zn Alloy Axial Fatigue Constant Strain Amplitude Mechanisms of Deformation Elevated Temperatures Strain Rate Grain Sizes						

INSTRUCTIONS

1. ORIGINATING ACTIVITY: Enter the name and address of the contractor, subcontractor, grantee, Department of Defense activity or other organization *(corporate author)* issuing the report.

2a. REPORT SECURITY CLASSIFICATION: Enter the overall security classification of the report. Indicate whether "Restricted Data" is included. Marking is to be in accordance with appropriate security regulations.

2b. GROUP: Automatic downgrading is specified in DoD Directive 5200.10 and Armed Forces Industrial Manual. Enter the group number. Also, when applicable, show that optional markings have been used for Group 3 and Group 4 as authorized.

3. REPORT TITLE: Enter the complete report title in all capital letters. Titles in all cases should be unclassified. If a meaningful title cannot be selected without classification, show title classification in all capitals in parenthesis immediately following the title.

4. DESCRIPTIVE NOTES: If appropriate, enter the type of report, e.g., interim, progress, summary, annual, or final. Give the inclusive dates when a specific reporting period is covered.

5. AUTHOR(S): Enter the name(s) of author(s) as shown on or in the report. Enter last name, first name, middle initial. If military, show rank and branch of service. The name of the principal author is an absolute minimum requirement.

6. REPORT DATE: Enter the date of the report as day, month, year, or month, year. If more than one date appears on the report, use date of publication.

7a. TOTAL NUMBER OF PAGES: The total page count should follow normal pagination procedures, i.e., enter the number of pages containing information.

7b. NUMBER OF REFERENCES: Enter the total number of references cited in the report.

8a. CONTRACT OR GRANT NUMBER: If appropriate, enter the applicable number of the contract or grant under which the report was written.

8b, 8c, & 8d. PROJECT NUMBER: Enter the appropriate military department identification, such as project number, subproject number, system numbers, task number, etc.

9a. ORIGINATOR'S REPORT NUMBER(S): Enter the official report number by which the document will be identified and controlled by the originating activity. This number must be unique to this report.

9b. OTHER REPORT NUMBER(S): If the report has been assigned any other report numbers *(either by the originator or by the sponsor)*, also enter this number(s).

10. AVAILABILITY/LIMITATION NOTICES: Enter any limitations on further dissemination of the report, other than those imposed by security classification, using standard statements such as:

(1) "Qualified requesters may obtain copies of this report from DDC."

(2) "Foreign announcement and dissemination of this report by DDC is not authorized."

(3) "U. S. Government agencies may obtain copies of this report directly from DDC. Other qualified DDC users shall request through

_____."

(4) "U. S. military agencies may obtain copies of this report directly from DDC. Other qualified users shall request through

_____."

(5) "All distribution of this report is controlled. Qualified DDC users shall request through

_____."

If the report has been furnished to the Office of Technical Services, Department of Commerce, for sale to the public, indicate this fact and enter the price, if known.

11. SUPPLEMENTARY NOTES: Use for additional explanatory notes.

12. SPONSORING MILITARY ACTIVITY: Enter the name of the departmental project office or laboratory sponsoring *(paying for)* the research and development. Include address.

13 ABSTRACT: Enter an abstract giving a brief and factual summary of the document indicative of the report, even though it may also appear elsewhere in the body of the technical report. If additional space is required, a continuation sheet shall be attached.

It is highly desirable that the abstract of classified reports be unclassified. Each paragraph of the abstract shall end with an indication of the military security classification of the information in the paragraph, represented as *(TS), (S), (C), or (U)*

There is no limitation on the length of the abstract. However, the suggested length is from 150 to 225 words.

14 KEY WORDS: Key words are technically meaningful terms or short phrases that characterize a report and may be used as index entries for cataloging the report. Key words must be selected so that no security classification is required. Identifiers, such as equipment model designation, trade name, military project code name, geographic location, may be used as key words but will be followed by an indication of technical context. The assignment of links, rules, and weights is optional.

Security Classification